Atmos. Meas. Tech. Discuss., https://doi.org/10.5194/amt-2019-100
Manuscript under review for journal Atmos. Meas. Tech.
Discussion started: 18 March 2019

Atmospheric Measurement Techniques Discussions

The importance of particle size distribution shape for triple-frequency radar retrievals of the morphology of snow

Shannon L Mason[1,2], Robin J Hogan[3,1], Christopher Westbrook[1], Stefan Kneifel[4], and Dmitri Moisseev[5,6]

[1]University of Reading, Reading, UK
[2]National Centre for Earth Observation, Reading, UK
[3]European Centre for Medium-range Weather Forecasts, Reading, UK
[4]University of Cologne, Cologne, Germany
[5]University of Helsinki, Helsinki, Finland
[6]Finnish Meteorological Institute, Helsinki, Finland

Correspondence: Shannon L. Mason (s.l.mason@reading.ac.uk)

Abstract. The accurate representation of ice particles is essential for both remotely-sensed estimates of cloud and precipitation and numerical models of the atmosphere. As it is typical in radar retrievals to assume that all snow is composed of unrimed aggregate snowflakes, both denser rimed snow and the mixed-phase cloud in which riming occurs may be under-diagnosed in retrievals, and therefore difficult to evaluate in weather and climate models. Recent experimental and numerical studies have yielded methods for using triple-frequency radar measurements to distinguish fractal aggregate snowflakes from more dense and homogeneous rimed particles.

In this study we investigate which parameters of the particle size distribution (PSD) and morphology of ice particles are most important to the triple-frequency radar signature of snow, in order to carry out an optimal estimation retrieval using triple-frequency Doppler radar observations. We represent a range of ice particle morphologies using a fractal model for aggregate snowflakes and homogeneous spheroids to represent rimed graupel-like particles, and modulate the prefactor and exponent of the particles' mass-size relations with a density factor. We find that for both fractal particles and homogeneous spheroids the PSD shape has a greater influence on the triple-frequency radar signature than the density factor, and show that the PSD shape must be allowed to vary to adequately constrain a triple-frequency radar retrieval of snow. We then demonstrate a novel triple-frequency Doppler radar retrieval of three parameters of the PSD as well as particle density, and show that the estimated snow rate, PSD and bulk density compare well against in situ observations at the surface. In a case study of compact rimed snow, we find that triple-frequency radar measurements provide a strong constraint on the estimation of PSD shape, but a relatively weak constraint on particle density, which we find can be more directly estimated from the Doppler velocity due to the relation between particle density and fallspeed. Including variations in PSD shape as well as particle morphology allows for a better representation of the triple-frequency radar signatures of rimed and unrimed snow, and suggests the potential for making new insights into the interaction between particles during aggregation and riming mechanisms. However, we find that improved representation of the PSD shape has a limited impact on improved estimates of snow rate from radar. The importance of the PSD shape to triple-frequency radar retrievals of snow suggests that further work is needed to account for variations in PSD shape before triple-frequency radar measurements can be used to better constrain particle morphology.

Atmos. Meas. Tech. Discuss., https://doi.org/10.5194/amt-2019-100
Manuscript under review for journal Atmos. Meas. Tech.
Discussion started: 18 March 2019

Atmospheric Measurement Techniques Discussions

1 Introduction

Remotely-sensed estimates of ice clouds and snow from spaceborne radars inform our understanding of key components of the global water and energy cycles. Both retrieval algorithms and numerical weather and climate models rely on a representation of the ice particle size distribution (PSD) and morphology, which are functions of the microphysical processes by which ice particles form, interact and grow. The processes of deposition, aggregation and riming may all contribute to the formation of a snowflake, and this growth history is encoded in the morphology of an ice particle. As riming requires the interaction of precipitating ice with supercooled liquid droplets in mixed-phase cloud layers which are difficult to diagnose, it has long been assumed that the majority of snow falls as unrimed pristine or aggregate snowflakes (Langleben, 1954); however, recent global active remote-sensing suggests that mixed-phase clouds are frequently associated with snow, especially over the ocean (Battaglia and Delanoë, 2013). Nevertheless, it has been typical to assume a fixed representation of the morphology and size distribution of ice particles, usually derived from measurements of unrimed aggregates (e.g. Delanoë and Hogan, 2008; Hogan et al., 2012). This means that many radar retrievals of snow do not represent particles which have grown by riming, a process which can contribute a significant fraction of the mass of snow (Mosimann, 1995; Grazioli et al., 2015; Tiira et al., 2016; Moisseev et al., 2017; von Lerber et al., 2017).

Radar retrievals that allow variation in the morphology of ice particles are therefore of significant interest, and the development of novel retrieval methods has been facilitated by measurement campaigns combining multiple-frequency radars and other remote-sensing instruments with in situ measurements of snow particle properties (e.g. Szyrmer and Zawadzki, 2014a; Petäjä et al., 2016). Doppler velocity measurements of the terminal fallspeed of snow have been used to constrain variations in particle density by which riming of snow, and the mixed-phase cloud in which it occurs, can be diagnosed (Mosimann, 1995; Szyrmer and Zawadzki, 2014a, b; Mason et al., 2018). Variations in the density of ice particles are also related to changes in their shape and structure—whether due to aggregation, riming or a combination of processes—which are reflected in their radar backscatter cross-sections (Leinonen and Szyrmer, 2015). Mason et al. (2018) formulated a single parameter modulating the density, shape and structure of ice particles which was retrieved in single- and dual-frequency Doppler radar retrievals, and was chiefly constrained by the mean Doppler velocity. This representation was based on a large database of ice particle mass- and area-size relations and insights from remote-sensed and in-situ measurements of snow events (Kneifel et al., 2015), but it remains to explore in more detail how the parameters controlling the size distribution and morphology of snow particles relate to one another and their radar scattering characteristics.

The relation between ice particle morphology and triple-frequency radar measurements emerges in a comparison of models for the radar backscatter cross-sections of ice particles (Kneifel et al., 2011). The triple-frequency radar 'signature' consists of two dual-wavelength ratios (DWRs) derived from radar measurements at 95, 35-GHz and a third frequency below 15-GHz, and provides a succinct means of evaluating the applicability of spheroidal particles as models for fractal aggregate snowflakes (Leinonen et al., 2012), revealing the fractal dimension of observed aggregates (Stein et al., 2015), and exploring

Atmos. Meas. Tech. Discuss., https://doi.org/10.5194/amt-2019-100
Manuscript under review for journal Atmos. Meas. Tech.
Discussion started: 18 March 2019


Atmospheric Measurement Techniques Discussions

their microphysical structure (Leinonen and Moisseev, 2015). Triple-frequency radar observations of rimed snow combining ground-based radar and in situ measurements (Kneifel et al., 2015) showed the apparent influence of increasing particle density on the triple-frequency radar signature, while a modelling study of the combined effects of growth by aggregation and riming related triple-frequency measurements to microphysical processes (Leinonen and Szyrmer, 2015). Combining triple-frequency and Doppler velocity information, Kneifel et al. (2016) used triple-frequency Doppler spectra to identify the spectral signatures of rimed and unrimed snow. The insights provided by triple-frequency radar techniques have contributed to the development of expanded scattering databases for representing and evaluating a wide range of ice particles (Kneifel et al., 2018).

The strong numerical and observational evidence that the triple-frequency radar signature reflects the density and structure of snow particles suggests the potential for retrievals in which some morphological parameters are constrained by triple-frequency radar measurements. Triple-frequency radar retrievals have been demonstrated in which the structure and density of ice particles are allowed to vary (Leinonen et al., 2018; Tridon et al., 2019); however, it is not yet clear which ice particle properties are best constrained by the triple-frequency radar measurements; Leinonen et al. (2018) found that a triple-frequency radar retrieval did not differ significantly from that of a dual-frequency retrieval, suggesting that the problem is over-constrained. To our knowledge, a triple-frequency Doppler retrieval of ice has not yet been described—this may have the advantages of estimating particle density constrained by Doppler velocity (as in Mason et al., 2018) and using triple-frequency radar signatures to constrain some parameters of particle morphology.

In this study we explore the potential for a triple-frequency Doppler radar retrieval using the optimal estimation framework Cloud Aerosol and Precipitation from mulTiple Instruments using a VAriational TEchnique (CAPTIVATE; Mason et al., 2018). In Section 2 we briefly describe the key components of the radar forward-model, and the remotely-sensed and in situ data used to perform and evaluate the retrieval. In Section 3 we then explore the effects of ice PSD and particle morphology parameters on the forward-modelled triple-frequency radar signatures of fractal and homogeneous spheroid models for aggregate snowflakes and graupel-like particles, respectively. In Section 4 we compare our models for snow particles against triple-frequency radar measurements from a case study of rimed and unrimed snow during Biogenic Aerosols—Effects of Clouds and Climate (BAECC) in Hyytiälä, Finland in 2014 (Petäjä et al., 2016). We demonstrate a triple-frequency Doppler radar retrieval in the rimed and unrimed snow in which key parameters of the PSD and particle morphology are retrieved, and evaluate the estimates against in situ measurements at the surface. In Section 5 we summarise our findings and make some concluding remarks.

2 Methods and data

We first describe the retrieved state variables and radar measurement variables (Section 2.1), then outline the radar and in situ measurements.

Atmos. Meas. Tech. Discuss., https://doi.org/10.5194/amt-2019-100
Manuscript under review for journal Atmos. Meas. Tech.
Discussion started: 18 March 2019

Atmospheric Measurement Techniques Discussions

2.1 Radar forward model and retrieval algorithm

We use the optimal estimation retrieval algorithm CAPTIVATE described by Mason et al. (2018). This framework has been developed for retrievals with the Doppler cloud profiling radar aboard EarthCARE (Illingworth et al., 2015), but is configurable for multiple radar instruments in ground-based and airborne, as well as spaceborne, applications. Here we describe the major components of the CAPTIVATE radar forward-model pertinent to ice and snow.

The ice PSD is the number of particles N of maximum dimension D, represented by the normalized gamma distribution

$$N(D) = N_w \frac{\Gamma(4)}{4^4} \frac{(4+\mu)^{4+\mu}}{\Gamma(4+\mu)} \frac{D}{D_0} \exp\left(-(4+\mu)\frac{D}{D_0}\right), \quad (1)$$

where N_w is the normalized number concentration, D_0 is the median volume diameter, Γ is the gamma function, and μ the shape parameter of the PSD (Testud et al., 2001; Illingworth and Blackman, 2002; Delanoë et al., 2005). While the majority of triple-frequency radar studies thus far have assumed the exponential PSD (i.e. $\mu = 0$), in situ measurements of snow at Hyytiälä include Gamma PSD shapes in the range $-2 < \mu < 5$ (Fig. 15 in Tiira et al., 2016). Modified 'universal' PSDs formulated to address the need for non-exponential distributions (Delanoë et al., 2005; Field et al., 2005, 2007) have been implemented in CAPTIVATE (Mason et al., 2018); however, in this study Gamma PSDs are used in order to explore the effects of accounting for PSDs broader ($\mu < 0$) and narrower ($\mu > 0$) than the exponential.

The morphology of the ice particles is represented by three parameters controlling their microphysical structure, density, and shape. The microphysical structure is represented in an approximation to the radar backscatter cross-section $\sigma(D)$ of each particle. In this study we use two approximations to represent the range of particle structures from aggregates snowflakes to graupel. Aggregate snowflakes are represented as fractal particles using the Self-Similar Rayleigh Gans Approximation (SSRGA; Hogan and Westbrook, 2014; Hogan et al., 2017) after the aggregate snowflake model of Westbrook et al. (2004). Heavily rimed graupel-like particles are represented using the T-matrix approximation for 'soft spheroids' composed of a homogeneous mixture of ice and air (e.g. Hogan et al., 2012). This approximation is not suited to representing aggregate snowflakes, but provides a good approximation to graupel (Leinonen and Szyrmer, 2015). The density factor r is a parameterisation described by Mason et al. (2018), which varies both the prefactor and exponent of the ice particle mass-size relation $m(D) = aD^b$, between that of the "aggregates of unrimed bullets, columns and side-planes" of Brown and Francis (1995) at $r = 0$ and that of spheroids of solid ice at $r = 1$. Mason et al. (2018) showed that this parameter allowed for simplified representation of a broad range of measured mass-size relations for particles along a continuum from unrimed aggregates to rimed snow, graupel, and hail. Finally, the shape of all particles is defined by horizontally-aligned oblate spheroids with axial ratio AR.

We note that in nature the structure, density and shape of snow particles are not independent. As discussed in more detail in Mason et al. (2018), the fractal or homogeneous distribution of mass through the volume of a particle is closely related to its density: the fractal structure of aggregates snowflakes is characterised by a mass-size relation with an exponent close to $b = 2$, while more homogeneous graupel and hail particles have mass-size relations with b approaching 3. The riming process by which aggregates accrete mass to become more graupel-like is also known to change the particle shape, with axial ratios increasing from more oblate snowflakes ($AR \approx 0.6$) to rounder graupel particles with $AR > 0.8$ (Li et al., 2018).

Atmos. Meas. Tech. Discuss., https://doi.org/10.5194/amt-2019-100
Manuscript under review for journal Atmos. Meas. Tech.
Discussion started: 18 March 2019

Atmospheric Measurement Techniques Discussions

2.1.1 State vector

As described in Mason et al. (2018), CAPTIVATE has been developed for radar-lidar-radiometer synergy from the upcoming EarthCARE satellite, and the retrieval of ice and snow follows the work of Delanoë and Hogan (2008) for radar-lidar synergy. The state vector is:

$$\mathbf{x} = \begin{pmatrix} \ln \alpha_{\mathrm{v}} \\ \ln N_0' \\ r' \end{pmatrix},$$

where the visible extinction coefficient α_{v} in the geometric optics approximation and primed number concentration N_0' are chosen so that prior estimate can be made as a function of atmospheric temperature (see Fig. 3 of Delanoë and Hogan, 2008). Retrieving both of these terms provides sufficient degrees of freedom to derive two parameters of the PSD, the median volume diameter and normalized number concentration; these more physically meaningful values, rather than the state variables, are reported in this study. The natural logarithms of most parameters are used to avoid non-physical negative values and to improve convergence, while the density index r' state variable is a function of the density factor such that r' is defined at all real values (Mason et al., 2018). To reduce the effect of measurement noise on the retrieval, the retrieved state variables are represented as the basis functions of a cubic spline (Hogan, 2007). The PSD shape, ice particle axial ratio and chosen model for ice particle structure and radar backscatter are configurable at runtime, but are assumed constant within each retrieval.

2.1.2 Measurement vector

The radar reflectivity factor (in linear units) at frequency f is given by

$$Z_f = \frac{\lambda_f^4}{\pi^5 |K_w|^2} \int_0^\infty \sigma_f(D)\, N(D)\, dD \tag{2}$$

where λ_f is the radar wavelength, K_w is the dielectric factor of water at cm wavelengths, and $\sigma_f(D)$ is the backscatter cross-section for a particle of maximum dimension D at the radar frequency. The dual-wavelength ratio (DWR) between frequencies f_1 and f_2 is then $\mathrm{DWR}_{f_1-f_2} = Z_{f_1}/Z_{f_2}$. Both radar reflectivity and DWR are reported in dB unless otherwise stated. While DWR quantities are reported here, the radar reflectivity factors at each frequency are used in the measurement vector.

Mean Doppler velocity is given by

$$V_f = \frac{\int_0^\infty v(D)\, \sigma_f(D)\, N(D)\, dD}{\int_0^\infty \sigma_f(D)\, N(D)\, dD}, \tag{3}$$

where the terminal velocity of an ice particle $v(D)$ assumes negligible vertical air motion, and positive values of mean Doppler velocity are toward the surface.

Atmos. Meas. Tech. Discuss., https://doi.org/10.5194/amt-2019-100
Manuscript under review for journal Atmos. Meas. Tech.
Discussion started: 18 March 2019

Atmospheric Measurement Techniques Discussions

The measurement vector for n radar frequencies is therefore given by

$$\mathbf{y} = \begin{pmatrix} Z_{\mathrm{f}_1} \\ \vdots \\ Z_{\mathrm{f}_n} \\ V_{\mathrm{f}_1} \\ \vdots \\ V_{\mathrm{f}_n} \end{pmatrix}.$$

In practice we may also perform retrievals using two or three radar frequencies, and use mean Doppler velocity at one radar frequency.

2.2 Radar and in situ measurements

Atmospheric Radiation Measurement second mobile facility (AMF2) Doppler radars at 10, 35 and 95-GHz were deployed at Hyytiälä, Finland during the Biogenic Aerosols—Effects on Clouds and Climate (BAECC) field campaign in 2014 (Petäjä et al., 2016). Radar measurements used here are at ~2 s temporal and ~30 m vertical resolution, and radar reflectivities have been corrected for gaseous and liquid attenuation. The specifications of the AMF2 radars, and their colocation, calibration and attenuation correction for triple-frequency radar measurements during BAECC 2014 are described in Kneifel et al. (2015).

In situ measurements of the snow at the surface are provided by the Particle Imaging Package (PIP) video disdrometer (Newman et al., 2009). PIP measurements and retrievals of parameters of the PSD and bulk particle density at 5 minute temporal resolution from Hyytiälä are described in Tiira et al. (2016) (also Moisseev et al., 2017; von Lerber et al., 2017). The method of moments is used to estimate the parameters of the Gamma distribution from the measured PSD (Moisseev and Chandrasekar, 2007).

The case study in Section 4 consists of approximately 25 minutes of zenith-pointing triple-frequency Doppler radar data from 22:53 to 23:18 UTC on 21 February 2014. The radar measurements are complemented by a radiosonde profile of atmospheric pressure, temperature and humidity which provides thermodynamic information for the retrieval.

3 Influences on the triple-frequency radar signature

In this section we use approximations to radar backscatter cross-section to explore the importance of ice particle morphology and size distribution on the triple-frequency radar signature. As described in Section 2.1.1, we represent ice particle morphology using parameters that control their microphysical structure, density and shape. We consider the range of particle structures by comparing two approximations to radar backscatter cross-sections: aggregate snowflakes are represented as fractal particles, and heavily rimed graupel-like particles as homogeneous spheroids. The density factor and the axial ratio control the mass-size relation and particle shape. The final parameter is the PSD shape, which is independent of the particle morphology, but affects the relative weighting given to particles across the size spectrum. Most studies of triple-frequency radar signatures of

Atmos. Meas. Tech. Discuss., https://doi.org/10.5194/amt-2019-100
Manuscript under review for journal Atmos. Meas. Tech.
Discussion started: 18 March 2019

Atmospheric Measurement Techniques Discussions

ice particles have assumed exponential PSDs (Kneifel et al., 2011; Leinonen et al., 2011; Kneifel et al., 2015; Leinonen and Moisseev, 2015; Leinonen and Szyrmer, 2015).

For a given particle morphology and PSD shape, the triple-frequency radar signature represents the values of DWR_{35-95} and DWR_{10-35} for a range of median volume diameters from 0.1 to 20 mm. The triple-frequency radar signatures for fractal particles (Fig. 1 a–c) and homogeneous spheroids (Fig. 1 d–f) are compared for a range of values of PSD shape (Fig. 1 a & d), density factor, (Fig. 1 b & e) and aspect ratio (Fig. 1 c & f). Intervals of median volume diameter in millimeters are labeled in (Fig. 1 a & d). The triple-frequency radar signatures overlay triple-frequency radar measurements from the case study considered in more detail later (Section 4); (Kneifel et al., 2015) showed that these data reflect distinct triple-frequency signatures. The curved signatures with high values of DWR_{10-35} correspond to large aggregate snowflakes, and the flatter signatures with higher values of DWR_{35-95} to compact, heavily rimed snow.

The triple-frequency radar signatures for fractal particles exhibit maxima in DWR_{35-95} between 8 and 12 dB at median volume diameters around 5 to 10 mm, before doubling back such that most curves are non-unique with DWR_{35-95} while DWR_{10-35} continues to increase with median particle size. This "hook" feature in the triple-frequency radar signature is characteristic of aggregates in theoretical and observational studies (e.g. Kneifel et al., 2015). The concavity of the hook feature increases with both PSD shape (Fig. 1 a) and density factor (Fig. 1 b). The triple-frequency radar signature is relatively insensitive to the axial ratio of the spheroidal particles (Fig. 1 c). The triple-frequency signatures differ due to changing values of particle density and PSD shape factor between median volume diameters of 2 mm and 8 mm, but converge outside this range. Increasing the PSD shape results in greater maximum values of DWR_{35-95}: while an exponential PSD reaches a maximum of around 9 dB at a median volume diameter around 7 mm, narrower PSDs reach DWR_{35-95} of up to 12 dB at median volume diameters around 5 mm. A smaller range of triple-frequency signatures is attributable to changes in the density factor: low-density fractal particles exhibit a maximum DWR_{35-95} of around 9 dB at 7 mm median volume diameter, and increase to around 11 dB for denser particles with $r > 0.4$.

The flat signatures of homogeneous spheroids reach greater values of DWR_{35-95} than fractal particles, even at relatively small median volume diameters of 3 to 4 mm. Both PSD shape and density affect a shift of the signature to the lower-right of the diagram; and unlike fractal particles, the signatures of homogeneous spheroids do not converge at large median volume diameters. The density factor tends to increase the DWR_{35-95} for homogeneous spheroids; however, the hook feature only becomes evident for high density factors at large median volume diameters.

Regardless of particle structure, the aspect ratio of the particles has a relatively minor influence on the triple-frequency signature. We therefore maintain the assumption of $AR = 0.6$ for all particles in this study, but note that uncertainty in this value contributes to uncertainties in the retrieval in other respects. For example, Mason et al. (2018) found that assuming $AR = 0.8$ leads to a roughly 20% increase in retrieved ice water content when compared to $AR = 0.6$. In situ measurements show that heavily rimed and graupel particles tend to have higher aspect ratios (e.g. Garrett et al., 2015; Li et al., 2018), so including this effect in future retrievals may help to constrain uncertainties in estimates of dense rimed snow.

The range of radar signatures is overlaid with the measured triple-frequency radar data from Hyytiälä; it is clear that neither fractal particles nor homogeneous spheroids can entirely represent the range of measured triple-frequency radar signatures,

Atmos. Meas. Tech. Discuss., https://doi.org/10.5194/amt-2019-100
Manuscript under review for journal Atmos. Meas. Tech.
Discussion started: 18 March 2019

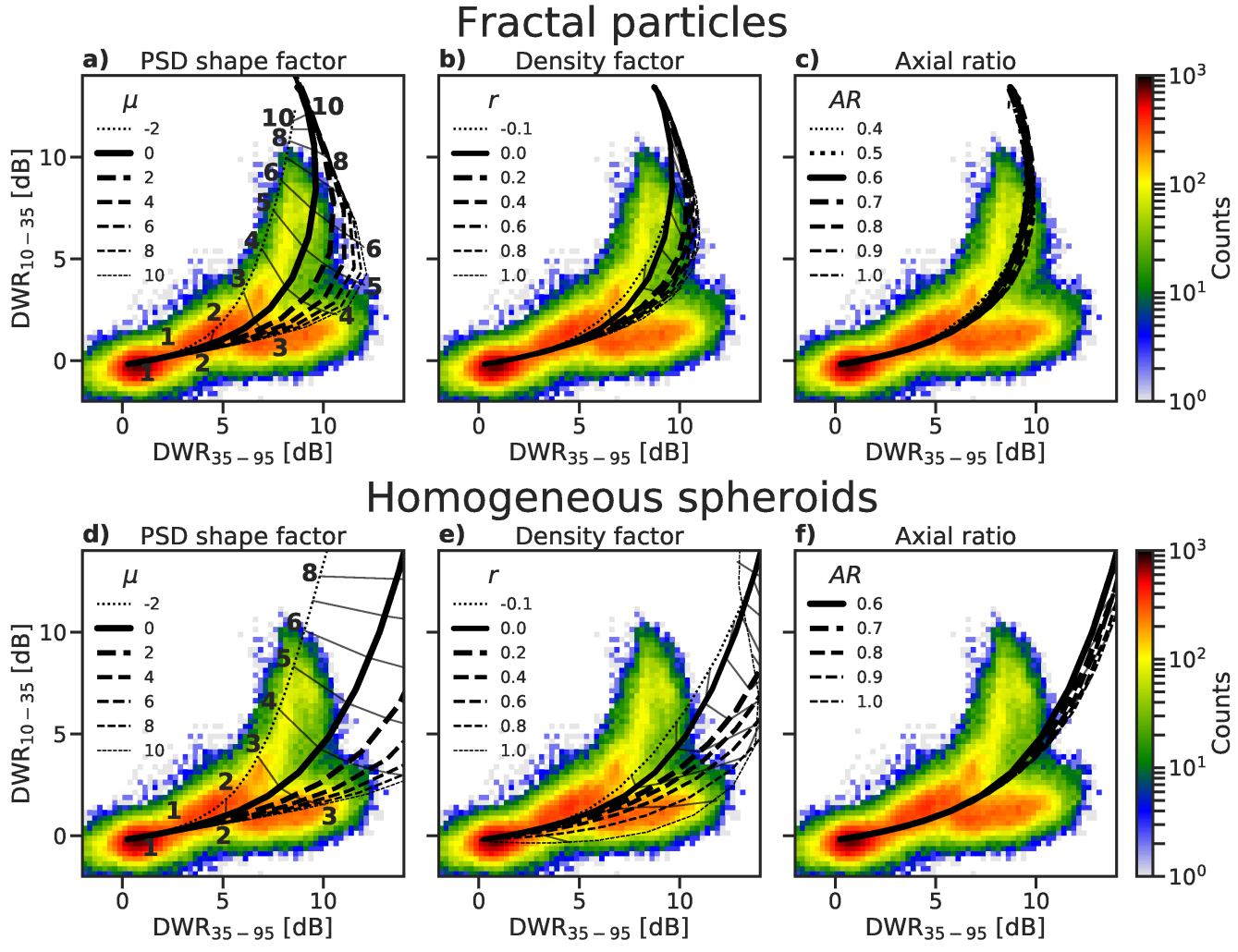

Figure 1. Simulated triple-frequency radar signatures for distributions of (a–c) fractal particles represented using SSRGA and (d–f) homogeneous ("soft") spheroids. Black lines illustrate radar signatures for a spectrum of PSDs with median volume diameters (values indicated in panels a and d) for different values of (a & d) PSD shape factor, (b & e) density factor, and (c & f) axial ratio. Lateral lines denote increments of median volume diameter in millimeters. Underlying the triple-frequency radar signatures are triple-frequency radar measurements from the 21 February 2014 case study at Hyytiälä, Finland (Kneifel et al., 2015).

Atmos. Meas. Tech. Discuss., https://doi.org/10.5194/amt-2019-100
Manuscript under review for journal Atmos. Meas. Tech.
Discussion started: 18 March 2019


Atmospheric Measurement Techniques Discussions

but also that there exists significant ambiguity between the radar signatures at all particle types, especially for median volume diameters less than around 3 mm. In an attempt to encompass this variability—acknowledging that the structure and density of ice particles are interrelated—Mason et al. (2018) formulated a hybrid representation which transitions from fractal particles at low density factors ($r < 0.2$) to represent unrimed and lightly rimed aggregates, to homogeneous spheroids at high densities ($r > 0.5$) representing graupel-like particles. Intermediate moderately rimed aggregates in the range $0.2 < r < 0.5$ ("hybrid particles" in Fig. 2 a) are represented by an external mixture of the backscatter cross-sections of the fractal and homogeneous models. More detailed parameterisations of this continuum may be achieved using the representation of a range of aggregates with different degrees of riming (Leinonen and Szyrmer, 2015), or fractal structures (Hogan et al., 2017), and should be the subject of further work.

For both fractal particles and homogeneous spheroids, the PSD shape has a greater influence on the triple-frequency signature than the particle density. The effect of the PSD shape is independent of the particle morphology, but results from changing the relative weighting of different parts of the particle size spectrum. To illustrate this effect, the radar backscatter cross-section ratio spectra for fractal particles and homogeneous spheroids with $r = 0$ and $AR = 0.6$ are compared in Fig. 2 (cf. the triple-frequency Doppler backscatter spectra studied by Kneifel et al., 2016). The ratios between radar backscatter cross-sections at 10–35-GHz and 35–95-GHz (Fig. 2 a) are shown alongside the volume-weighted particle size distributions for selected PSDs (Fig. 2 b): the exponential PSD (Marshall and Palmer, 1948), and PSDs measured during the pre-frontal and frontal snow regimes of the 21 February 2014 case at Hyytiälä, Finland, which is considered in more detail in Section 4. The frontal snow regime fits a broader Gamma PSD ($\mu = -1$), and the prefrontal rimed snow a narrower PSD ($\mu = 5$). As radar measurements relate to PSD-weighted integrals of the radar backscatter spectra by (1), the triple-frequency signature is strongly influenced by the median volume diameter and shape parameters of the PSD, with the PSD shape modulating the relative influence of spectral features close to the median volume diameter. As the median volume diameter approaches the onset of non-Rayleigh scattering at 95-GHz (around 3 mm), DWR_{35-95} increases, creating the initial horizontal part of the triple-frequency radar signatures of both fractal particles and homogeneous spheroids; correspondingly, at the onset of non-Rayleigh scattering at the 35-GHz (around 8 mm) there is a shift to larger values of DWR_{10-35}, and a vertical uptick in the triple-frequency diagram. For fractal particles (dashed lines Fig. 2 a) there is a clear distinction between the parts of the spectrum dominated by non-Rayleigh scattering at 95- and 35-GHz: the decrease in the 35–95-GHz backscatter cross-section ratio at median diameters greater than around 6–8 mm results in the "bending-back" part of the hook feature in the triple-frequency signature, which occurs at smaller median diameters for narrower PSD shapes (Fig. 1 a). For homogeneous spheroids (solid lines in Fig. 2 a) the many narrow features of the backscatter cross-section ratio spectra are smoothed out, resulting in a flatter triple-frequency radar signature. This illustrates how a narrower PSD will increase the weight given to particles closest to the median volume diameter, exaggerating the effects of nearby features of the radar backscatter spectra and deepening the hook feature characteristic of fractal particles as PSD shape increases. Conversely, broader PSDs have the effect of smoothing over the spectral features, producing an earlier onset of high values of DWR_{10-35} and a shallower hook feature for fractal particles.

We may therefore add to the diagram for the triple-frequency radar signature proposed in Kneifel et al. (2015) to include the effect of PSD shape as well as particle density (Fig. 3). This reflects a significant insight into the interpretation of triple-

Atmos. Meas. Tech. Discuss., https://doi.org/10.5194/amt-2019-100
Manuscript under review for journal Atmos. Meas. Tech.
Discussion started: 18 March 2019

Atmospheric Measurement Techniques Discussions

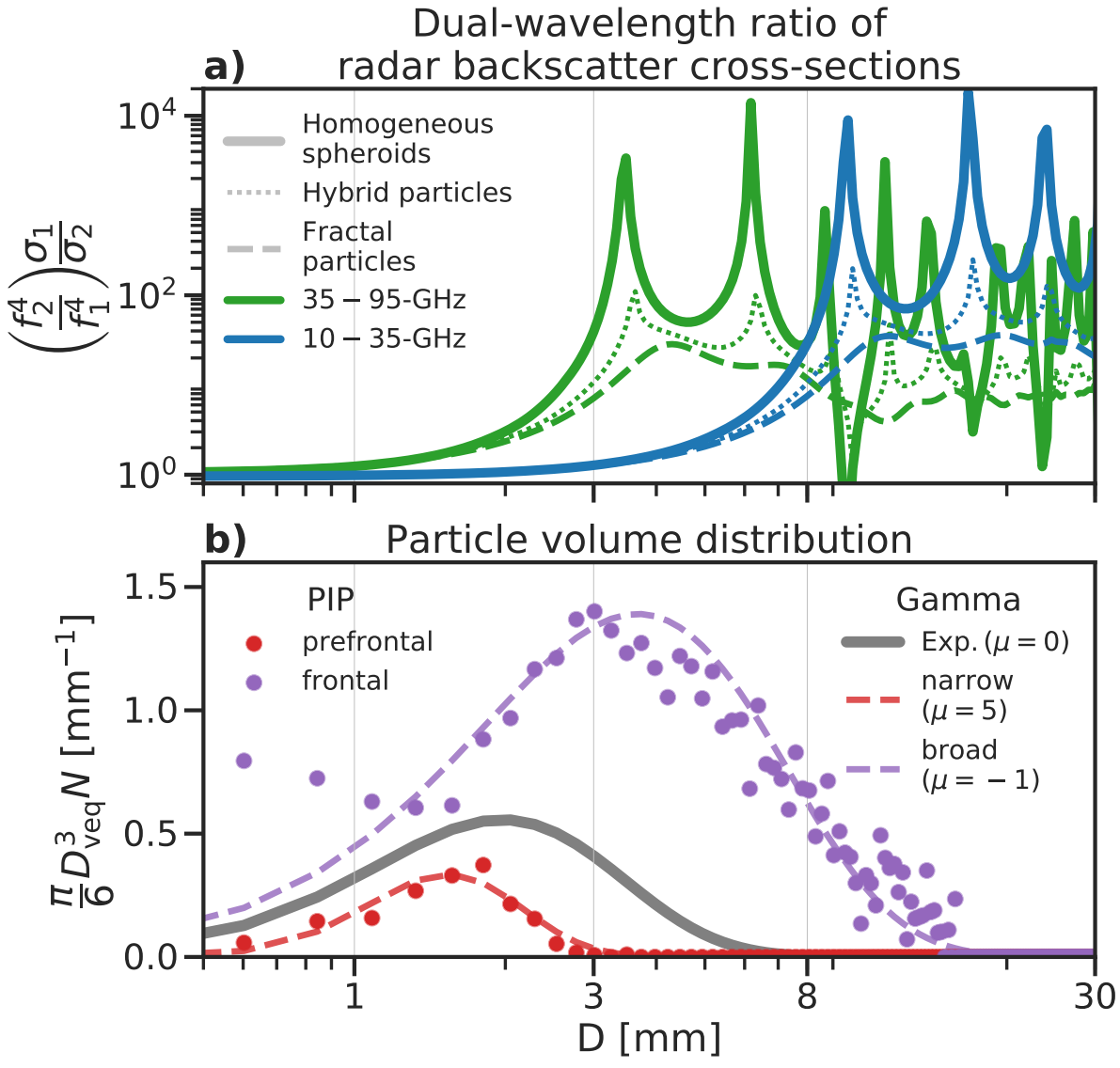

Figure 2. (a) Normalized backscatter cross-section ratios at 10–35-GHz and 35–95-GHz bands for fractal particles and homogeneous spheroids, on the same size spectrum as (b) the volume-weighted PSD measured in situ during the prefrontal and frontal regimes and Gamma PSDs fit to the same regimes, and an exponential ($\mu = 0$) PSD. The backscatter cross-section ratios of the "hybrid" particles in (a) illustrate the transition between fractal (SSRGA) and homogeneous or "soft" spheroid approximations for intermediate density factors between $0.2 < r < 0.5$ as described in Mason et al. (2018).

Atmos. Meas. Tech. Discuss., https://doi.org/10.5194/amt-2019-100
Manuscript under review for journal Atmos. Meas. Tech.
Discussion started: 18 March 2019

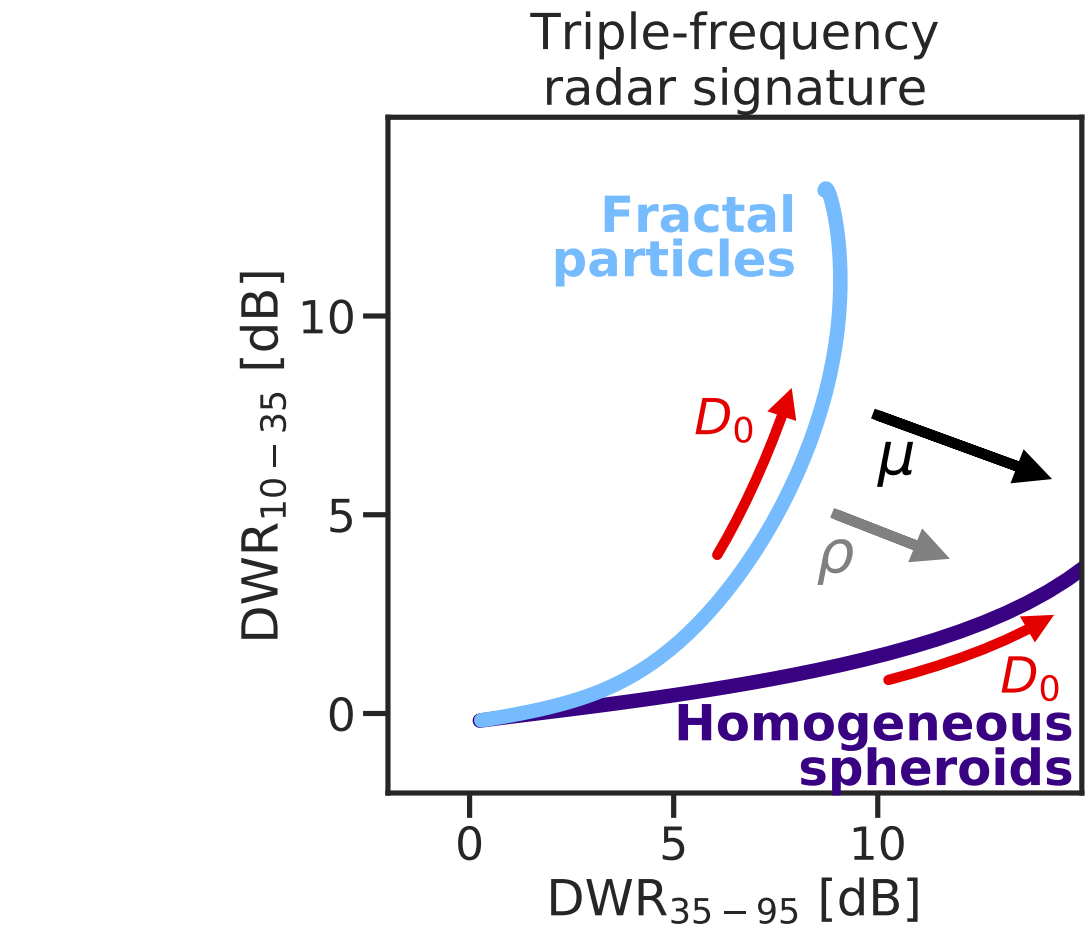

Figure 3. A schematic for the parameters affecting the triple-frequency radar signature of a spectrum of ice particles. In addition to the median volume diameter and density, the effects of particle structure and PSD shape are illustrated (cf. Kneifel et al., 2015).

frequency radar signatures, as it is possible that the observed range of measurements Kneifel et al. (2015) are attributable to the combined effects of increased density due to riming and a narrow PSD. It is not apparent to which degree these parameters are independent of one another, although Tiira et al. (2016) found only a weak relation between the bulk density and PSD shape factor estimated from PIP measurements at Hyytiälä. This poses a challenge when seeking to retrieve the morphology of particles from the triple-frequency radar measurements, a problem we will explore further in the next section.

4 Case study

In this section we revisit one of the triple-frequency radar case studies from Hyytiälä, Finland, explored by Kneifel et al. (2015). The 21 February 2014 case has been widely studied with remote-sensed and in situ observations because it includes

Atmos. Meas. Tech. Discuss., https://doi.org/10.5194/amt-2019-100
Manuscript under review for journal Atmos. Meas. Tech.
Discussion started: 18 March 2019


Atmospheric Measurement Techniques Discussions

the transition from heavily rimed to unrimed snow during the passage of a front. The 25-minute period of triple-frequency Doppler radar measurements (Figure 4) are separated into prefrontal (22:53 to 23:03 UTC) and frontal (23:03 to 23:18 UTC) regimes. Kneifel et al. (2015) showed that the onset of unrimed frontal snow corresponded to the emergence of the distinct hook feature in the triple-frequency signature, simultaneous with a reduction in particle fallspeeds observed both in situ and by mean Doppler velocity. Mason et al. (2018) exploited the Doppler velocity to constrain an estimate of the density factor in the context of single- and dual-frequency radar retrievals of a longer time series of the same case. Here we use the case study to consider the importance of the PSD to the triple-frequency signature (Section 4.1), and then attempt a retrieval of particle density and PSD shape from triple-frequency Doppler radar measurements (Section 4.2).

4.1 Triple-frequency radar signatures

In Section 3 we showed that the PSD shape has a greater influence on the triple-frequency radar signature than the density factor, but we did not consider the expected range of observed values for each of these parameters. Here we use in situ and remote-sensed measurements from the case study to explore the range of size distributions and particle morphologies that best explain the observed triple-frequency radar signatures.

We make a coarse distinction between the prefrontal regime before 23:03 UTC, and the frontal regime thereafter. Triple-frequency radar measurements (Fig. 4) show an increase in 10 and 35-GHz radar reflectivities with the onset of frontal snowfall, while the mean Doppler velocity nearest the surface decreases from around $2\,\mathrm{m\,s^{-1}}$ before the front arrives, to around 1 to $1.5\,\mathrm{m\,s^{-1}}$ during the frontal regime.

As a check on the representation of particle properties and radar scattering assumptions within CAPTIVATE, we evaluate the capability to reproduce triple-frequency radar signatures that resemble the triple-frequency radar measurements of rimed and unrimed snow during the prefrontal and frontal snow regimes. Previous analyses of in situ measurements and remote-sensed retrievals of the density factor can be used to confirm that the forward model captures the particle properties as well as the triple-frequency radar signatures.

The triple-frequency radar measurements below 2 km in the prefrontal regime are coloured by the average mean Doppler velocity, and contours at the 10 th, 50 th and 90 th percentiles indicate the frequency of the triple-frequency radar measurements (Fig. 5a). The rimed prefrontal snow is characterised by a flat triple-frequency signature in which DWR_{35-95} is between 5 and 11 dB, with DWR_{10-35} less than 2 dB, and mean Doppler velocities between 1.5 and $2\,\mathrm{m\,s^{-1}}$, consistent with dense rimed particles. The radar measurements are overlaid with triple-frequency radar signatures for homogeneous spheroids with a range of median volume diameters, PSD shapes and density factors. The bulk of the prefrontal snow corresponds to the triple-frequency radar signatures of homogeneous spheroids with a density factor of $r = 0.5$, consistent with compact graupel-like particles retrieved by Mason et al. (2018); and a PSD shape of $\mu = 5$, which was measured at the surface during this period (Fig. 2). Most of the measurements correspond to median volume diameters between 2 and 3 mm, consistent with PIP measurements during this period (Kneifel et al., 2015, and shown later in Fig. 8e.).

The frontal snow regime (Fig. 5b) exhibits the hook feature characteristic of unrimed aggregates, with most measurements of DWR_{35-95} between 5 and 10 dB and DWR_{10-35} up to around 8 dB. In contrast to the rimed prefrontal snow, this regime

Atmos. Meas. Tech. Discuss., https://doi.org/10.5194/amt-2019-100
Manuscript under review for journal Atmos. Meas. Tech.
Discussion started: 18 March 2019

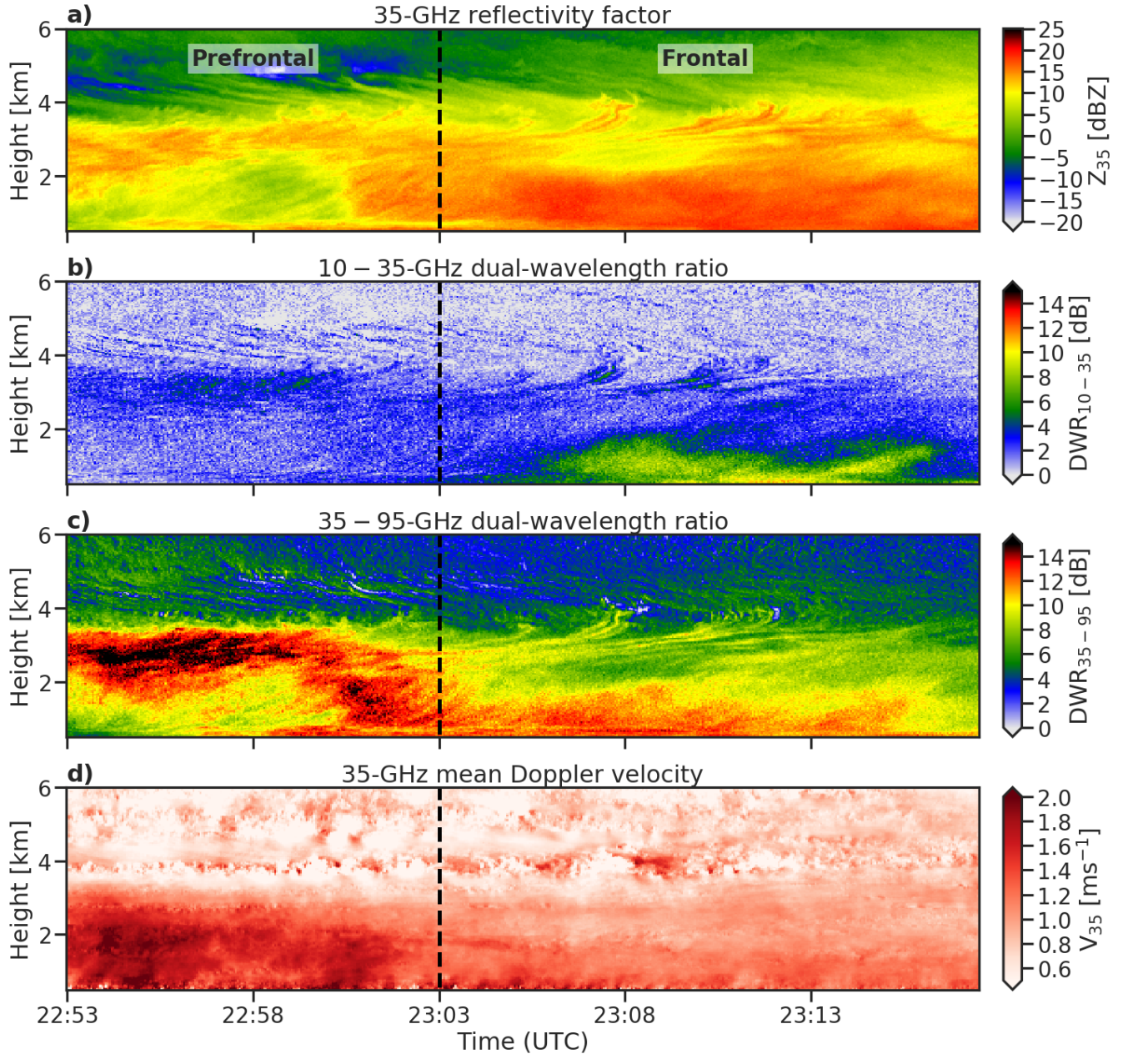

Figure 4. Triple-frequency Doppler radar measurements from the February 21 2014 case study at Hyytälä, Finland. (a) 35-GHz radar reflectivity, (b) 10–35-GHz dual wavelength ratio, (c) 35–95-GHz dual wavelength ratio, and (d) 35-GHz mean Doppler velocity. Dashed lines mark the transition between the prefrontal and frontal snowfall regimes.

Atmos. Meas. Tech. Discuss., https://doi.org/10.5194/amt-2019-100
Manuscript under review for journal Atmos. Meas. Tech.
Discussion started: 18 March 2019

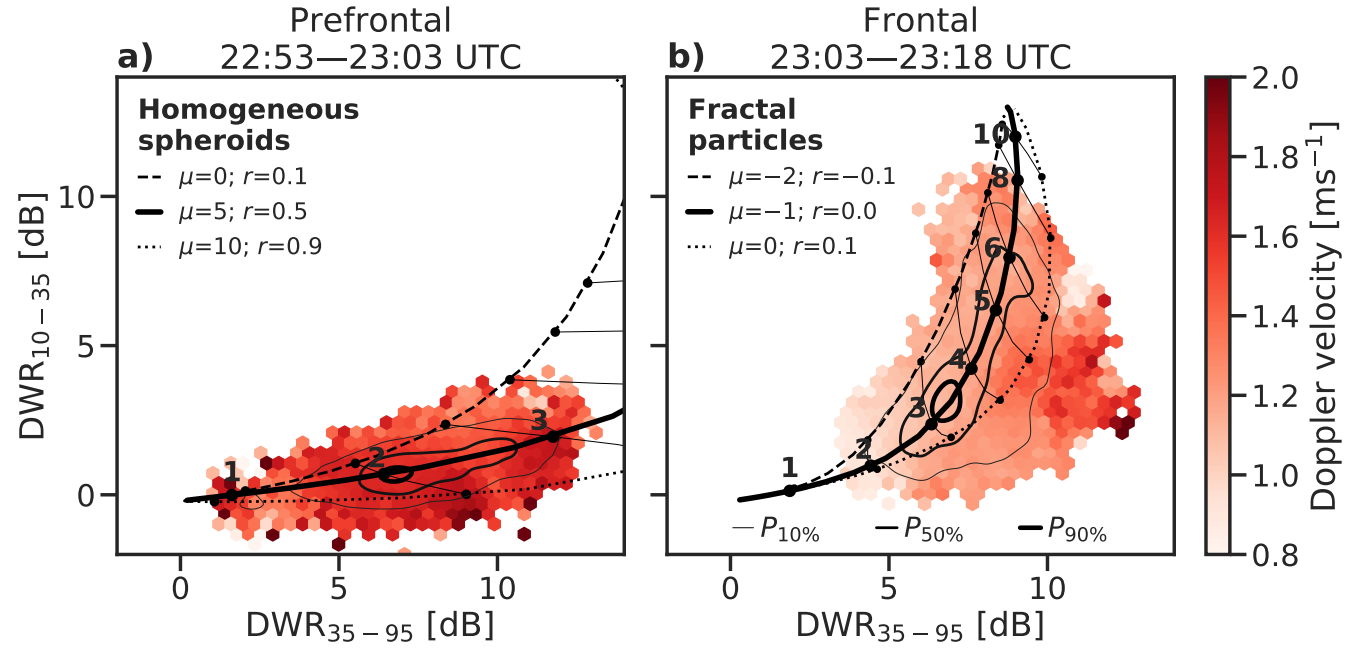

Figure 5. Triple-frequency radar measurements below 2 km above ground level in the (a) prefrontal and (b) frontal snow regimes of the 21 February 2014 case at Hyytiälä, Finland. Triple-frequency radar measurements are coloured by the corresponding mean Doppler velocity, and frequency of occurrence is indicated with black contours at the 10th, 50th and 90th percentiles. Overlaid are triple-frequency radar signatures for (a) homogeneous spheroids and (b) fractal particles with a range of values of PSD shape and density factor that encompass the most frequent triple-frequency radar measurements. Increments of median volume diameter are labelled in millimeters.

exhibits lower mean Doppler velocities between 1 and 1.5 m s^{-1}, but includes some triple-frequency radar measurements at higher values of DWR_{35-95} greater than 10 dB and mean Doppler velocities greater than 1.5 m s^{-1}, suggesting that some rimed particles persist after 23:03 UTC. The most frequent triple-frequency radar measurements are a good fit to fractal particles with a PSD shape with $\mu = -1$, which was measured in situ during the frontal regime; and a density factor of $r = 0$, corresponding to unrimed aggregate snowflakes. The triple-frequency radar measurements correspond to fractal particles with median volume diameters as small as 1.5 mm and as large as 8 mm, but the majority of the data suggest median diameters between 3 and 5 mm, which is consistent with in situ measurements at the surface (Fig. 8e).

Comparing our particle models parameterised by density factor and PSD shape against measured triple-frequency radar measurements, it is evident that the rimed prefrontal snow is well-represented by a narrow PSD comprising of dense graupel-like particles with a median volume diameter around 1 to 2 mm. In contrast, the frontal snow corresponds to a broad distribution of large unrimed aggregates with median volume diameters between 3 mm and 8 mm. The fit to triple-frequency radar signatures requires a representation of the PSD shape, particle density and microphysical structure, illustrating that the PSD shape is key to resolving the triple-frequency radar signatures of snow.

Atmos. Meas. Tech. Discuss., https://doi.org/10.5194/amt-2019-100
Manuscript under review for journal Atmos. Meas. Tech.
Discussion started: 18 March 2019

Atmospheric Measurement Techniques Discussions

4.2 Triple-frequency radar retrieval

In this section we perform an optimal estimation retrieval constrained by triple-frequency Doppler radar measurements. Mason et al. (2018) used a dual-frequency radar reflectivity to constrain two parameters of the PSD, while the density factor was constrained by mean Doppler velocity at one radar frequency. Following the studies of Leinonen et al. (2018) and Tridon et al. (2019), we are interested in whether the triple-frequency radar measurments can be used to constrain a retrieval of particle density, or if—given the evidence presented above—it will be essential to include information about the PSD shape in order to satisfy the triple-frequency constraint. If the major parameters controlling the triple-frequency signature were represented within a radar forward-model, an optimal estimation retrieval could be made to estimate those parameters, if adequately constrained by the measurements. With a secondary means of estimating the particle density from the mean Doppler velocity, we can compare estimates of particle density based on their ability to forward-model the measured mean Doppler velocity.

We perform retrievals assimilating a variety of radar measurements in order to compare their respective contributions. The default retrieval combines radar reflectivity at 10, 35 and 95-GHz and mean Doppler velocity at 35-GHz ($Z_{10,35,95}\,V_{35}$), which represents the full available measurement vector. To test the capability to retrieve the particle density from triple-frequency radar reflectivity factors, we also make a retrieval which does not assimilate Doppler velocity (i.e. $Z_{10,35,95}$); and to test the contribution of the third radar frequency, we test dual-frequency retrievals (i.e. $Z_{10,35}\,V_{35}$ and $Z_{35,95}\,V_{35}$). Reducing the number of measurements assimilated may lead to a more challenging inverse retrieval problem, wherein either the measurement vector provides insufficient constraint on an estimate of the state vector, or the state space does not include a solution that satisfies all of the measurements.

The quality of the retrieval may be illustrated by comparing the measurements against those forward-modelled from the retrieved state. We take representative profiles from each snow regime: a prefrontal profile characterised by rimed snow (23:00 UTC; Fig. 6), and a frontal profile dominated by large unrimed aggregates (23:10 UTC; Fig. 7). The profiles of retrieved variables are shown in the supplementary material.

Comparing retrievals of the prefrontal profile with an exponential PSD (Fig. 6 a–d), it is evident that the triple-frequency retrievals $Z_{10,35,95}\,V_{35}$ and $Z_{10,35,95}$ are not able to satisfy all three profiles of radar reflectivity simultaneously, with errors of 1 to 2 dB, while the dual-frequency radar retrievals $Z_{35,95}\,V_{35}$ and $Z_{10,35}\,V_{35}$ are able to satisfy the assimilated frequencies, but exhibit large errors in the remaining frequency (e.g. up to 4 dB in forward-modelled DWR_{10-35} for $Z_{35,95}\,V_{35}$). $Z_{10,35}\,V_{35}$ and $Z_{35,95}\,V_{35}$ are both well-constrained, and the profiles forward-modelled by $Z_{10,35,95}\,V_{35}$ resemble a compromise between the 95 and 10-GHz constraints. The retrievals assimilating Doppler velocity have adequate constraints on the density factor to represent the observed increase in mean Doppler velocity below around 3 km above ground level. $Z_{10,35,95}$ is similar to $Z_{10,35,95}\,V_{35}$ in terms of radar reflectivity, but the observed increase in mean Doppler velocity below $2\,\mathrm{km}$ above ground level is not resolved at all without assimilating the mean Doppler velocity.

As shown in Section 4.1, the triple-frequency radar measurements in the prefrontal regime are best represented with narrow PSDs with $\mu > 5$, consistent with in situ measurements at the surface. We therefore repeat the CAPTIVATE retrievals

Atmos. Meas. Tech. Discuss., https://doi.org/10.5194/amt-2019-100
Manuscript under review for journal Atmos. Meas. Tech.
Discussion started: 18 March 2019

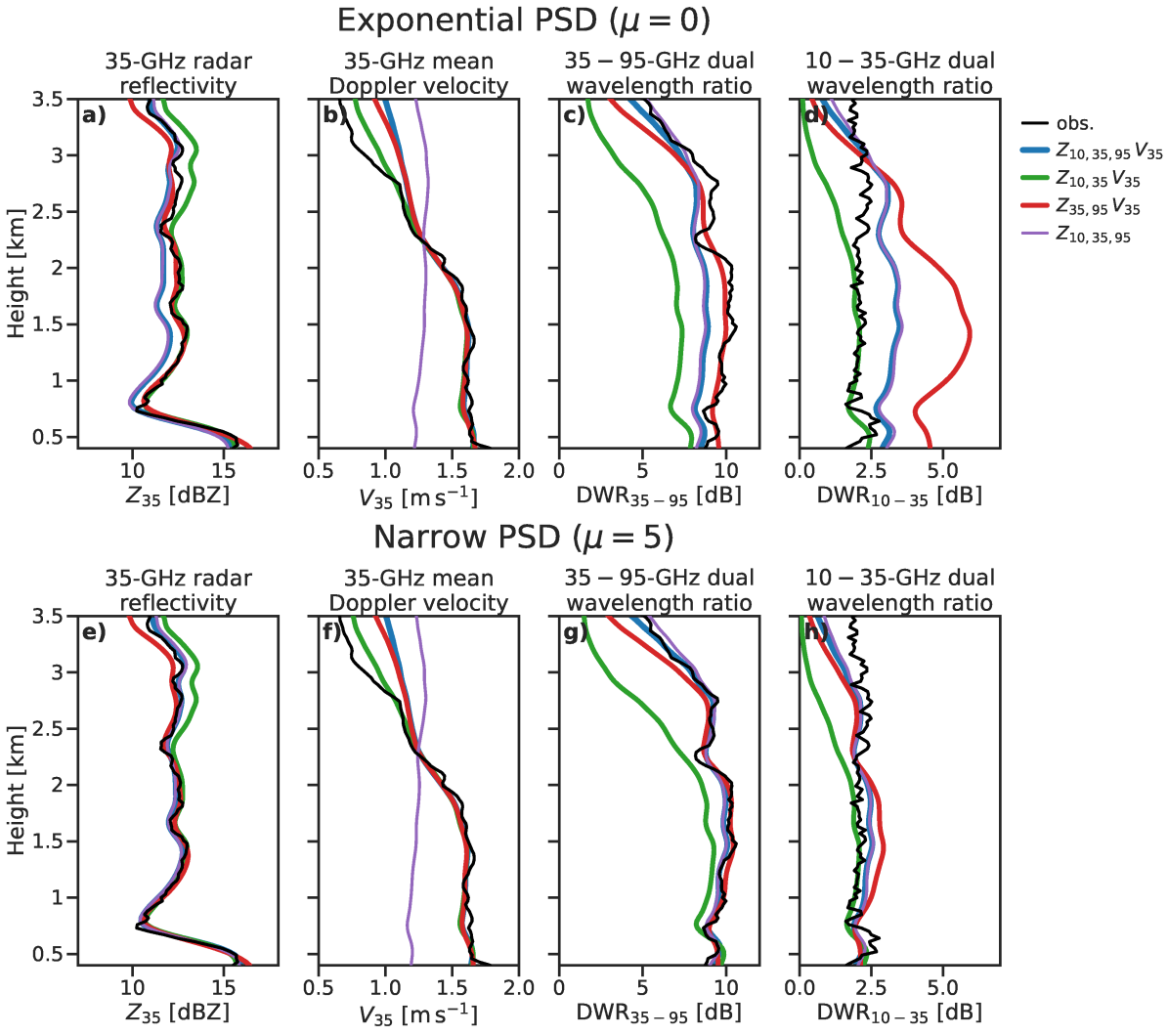

Figure 6. Profiles of observed and forward-modelled radar variables for retrievals of a selected profile during the prefrontal snow regime. Retrievals assuming (a–d) an exponential PSD are compared against those with (e–h) a narrow PSD with $\mu = 5$.

Atmos. Meas. Tech. Discuss., https://doi.org/10.5194/amt-2019-100
Manuscript under review for journal Atmos. Meas. Tech.
Discussion started: 18 March 2019

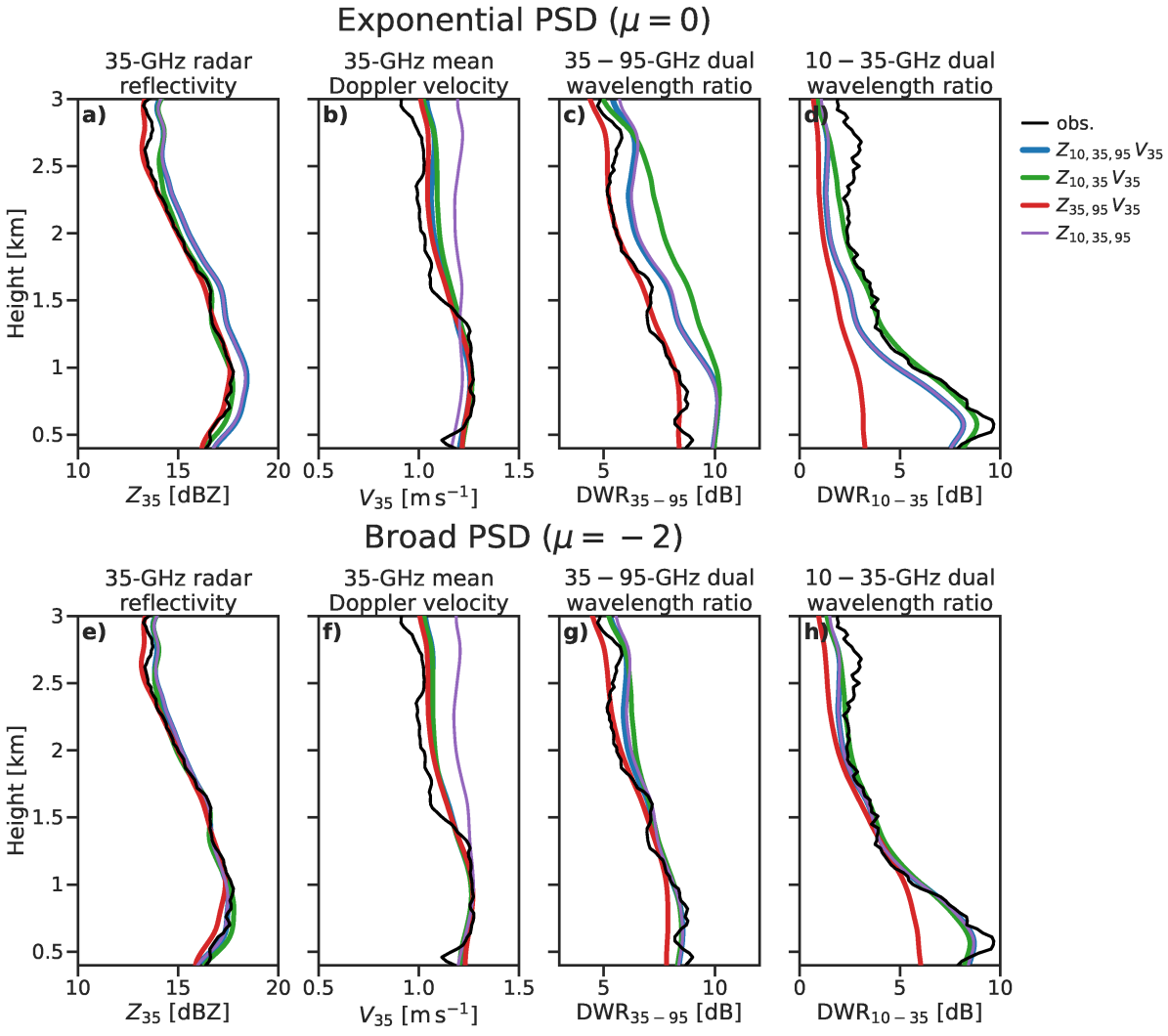

Figure 7. Profiles of observed and forward-modelled radar variables for retrievals of a selected profile during the frontal snow regime. Retrievals assuming (a–b) an exponential PSD are compared against those with (e–h) a broad PSD with $\mu = -2$.

Atmos. Meas. Tech. Discuss., https://doi.org/10.5194/amt-2019-100
Manuscript under review for journal Atmos. Meas. Tech.
Discussion started: 18 March 2019

Atmospheric Measurement Techniques Discussions

with constant $\mu = 5$ rather than $\mu = 0$ (Fig. 6 e–h). The forward-modelled profiles of radar reflectivity are considerably better constrained by the measurements in this retrieval: $Z_{10,35,95}\,V_{35}$ especially is very close to all the observations. The exception is that the retrieval does not match the 10-GHz reflectivity factor above around 3 km; it is likely that the PSD shape changes through this level, where the onset of the riming process is evident from increased mean Doppler velocities, and where layers of supercooled liquid have been identified in the Doppler spectra (Kalesse et al., 2016). The profiles of radar reflectivity of the dual-frequency retrievals are also better-constrained when a narrower PSD is assumed; however, it is not evident that the triple-frequency radar measurements provide any constraint on the density factor of $Z_{10,35,95}$: the forward-modelled mean Doppler velocity is unchanged.

Retrievals of the profile of unrimed frontal snow (Fig. 7) show similar results: when an exponential PSD is used, $Z_{10,35,95}\,V_{35}$ exhibits errors of up to 2 dB in the profiles of radar reflectivity. The retrieval is over-constrained with respect to triple-frequency radar measurements, as the state space does not allow for the triple-frequency radar signature of the large aggregates to be represented. A significant difference between the frontal and the prefrontal profiles is that all retrievals are able to represent the observed profile of mean Doppler velocity below about 1.5 km, showing that the prior density factor of $r = 0$ makes an accurate estimate of the terminal fallspeed of unrimed aggregate particles, provided their size is well-constrained by dual-frequency radar measurements—even when mean Doppler velocity measurements are not assimilated. Above 1.5 km, $Z_{10,35,95}$ over-estimates the mean Doppler velocity by around 0.2 m s^{-1}. As for the prefrontal profile, all of the retrievals are better able to represent the triple-frequency radar measurements when a non-exponential PSD is used; assuming a broader PSD with $\mu = -2$ results in consistently better-constrained retrievals at all three radar frequencies.

These results indicate that, at least as the retrieval is configured here, triple-frequency radar measurements are insufficient to constrain a retrieval of the density factor. This is consistent with the results of Leinonen et al. (2018), wherein the retrieved prefactor of the particle mass-size relation was relatively insensitive to the triple-frequency radar measurements. Instead, the mean Doppler velocity provides an effective constraint on the density of rimed snow, as in Mason et al. (2018). Furthermore, we have shown that the retrieval may be ill-posed if all ice is assumed to have an exponential PSD: that is, because the PSD shape has more a significant influence on the triple-frequency radar signature than the density of ice particles, it may not be possible to retrieve a state vector that satisfies all three radar frequencies unless the PSD shape can also be estimated.

We have shown that over-constrained retrievals in both the prefrontal and frontal profiles were improved by using in situ measurements to update the PSD shape, which is assumed constant within CAPTIVATE retrievals but can be configured at runtime. Further, we have confirmed that our models for aggregate snowflakes and graupel-like particles allow for a good representation of their triple-frequency radar signatures when both density and PSD shape are modified. Within an optimal estimation retrieval it therefore should be possible to minimise errors in the forward-modelled profiles of triple-frequency radar measurements to constrain the PSD shape in addition to the median volume diameter and normalized number concentration, which are well-constrained in dual-frequency retrievals. While CAPTIVATE is not currently configured to easily retrieve the PSD shape as a state variable, we can carry out a pseudo-retrieval by running $Z_{10,35,95}\,V_{35}$ retrievals in which PSD shape is assumed to take integer values from $\mu = -2$ to $\mu = 10$. The pseudo-retrieval is made by selecting the value of PSD shape that minimises the error in forward-modelled DWR_{35-95} and DWR_{10-35} between 400 and 600 m above ground level (Fig. 8a &

Atmos. Meas. Tech. Discuss., https://doi.org/10.5194/amt-2019-100
Manuscript under review for journal Atmos. Meas. Tech.
Discussion started: 18 March 2019


Atmospheric Measurement Techniques Discussions

b); the state vector is linearly interpolating between the retrieved state vectors at the retrieved value of PSD shape, giving an estimate of the other retrieved quantities when the PSD shape is retrieved (Fig. 8 d–g). To reduce noise in the pseudo-retrieval the minimisation is carried out at a smoothed temporal resolution of 15 s.

The retrieved timeseries of PSD (Fig. 8c) is consistent with that measured at the surface, with PSD shapes from $3 < \mu < 10$ reflecting narrow size distributions of snowfall in the prefrontal regime, and transitioning to broader PSDs with $-2 < \mu < 0$ after around 23:05 UTC. Prior to 23:00 UTC the retrieved PSD noisy, with high uncertainties reflecting the increasingly weak distinctions between PSD shapes in the timeseries of forward-modelled DWR (Fig. 8a & b); this is because, as observed in Figs. 1 & 2, the triple-frequency signatures converge at median volume diameters less than around 2 mm, the sizes at which non-Rayleigh scattering is insignificant at 95-GHz. Comparison to the PSD shape estimated from PIP measurements is especially difficult when snow is dominated by small particles, where truncation effects on the use of the method of moments to estimate parameters of the PSD become significant.

The triple-frequency retrievals of snow rate, median volume diameter, number concentration and bulk density at 500 m are all reasonably well-matched to in situ measurements at the surface, given the differences in temporal resolution between the two estimates. The snow rate is very similar to that measured at the surface, while the median volume diameters are overestimated by around 50 % in the period of heaviest frontal snowfall, and retrieved normalized number concentration is within a factor of two of the PIP estimates. While retrieving PSD shape enables a significant improvement in the representation of triple-frequency radar measurements, we note that this has little impact on the retrieved snow rate or bulk density when compared to a retrieval that assumes an exponential PSD. Retrieving a broad PSD in the frontal snowfall results in median volume diameters roughly 1 mm greater; normalised number concentrations are as much as a factor of two lower in the prefrontal regime, and up to a factor of two greater toward the end of the frontal regime.

5 Discussion and conclusions

It has been well established in numerical and experimental studies that the triple-frequency radar signature of snow can provide insights into the structure, size and density of ice particles (Kneifel et al., 2011; Leinonen et al., 2012; Kneifel et al., 2015; Stein et al., 2015). Triple-frequency radar studies (with the exception of Leinonen et al., 2012) have typically assumed exponential size distributions—an assumption also commonly made in radar retrievals because uncertainties in the PSD shape have a relatively weak influence on estimates of ice water content (e.g. Delanoë et al., 2005). In this study, we have shown that the PSD shape has an important effect on the triple-frequency radar signature by exaggerating or smoothing over features in the radar backscatter spectra, and that this influence can be more significant than changes in particle density. Using ground-based triple-frequency radar measurements alongside in situ measurements of particle properties at the surface, we showed that including variations in the PSD shape permitted more accurate representations of the measured triple-frequency radar signatures of graupel-like particles modelled as homogeneous spheroids, and of unrimed aggregate snowflakes modelled as fractals.

Atmos. Meas. Tech. Discuss., https://doi.org/10.5194/amt-2019-100
Manuscript under review for journal Atmos. Meas. Tech.
Discussion started: 18 March 2019

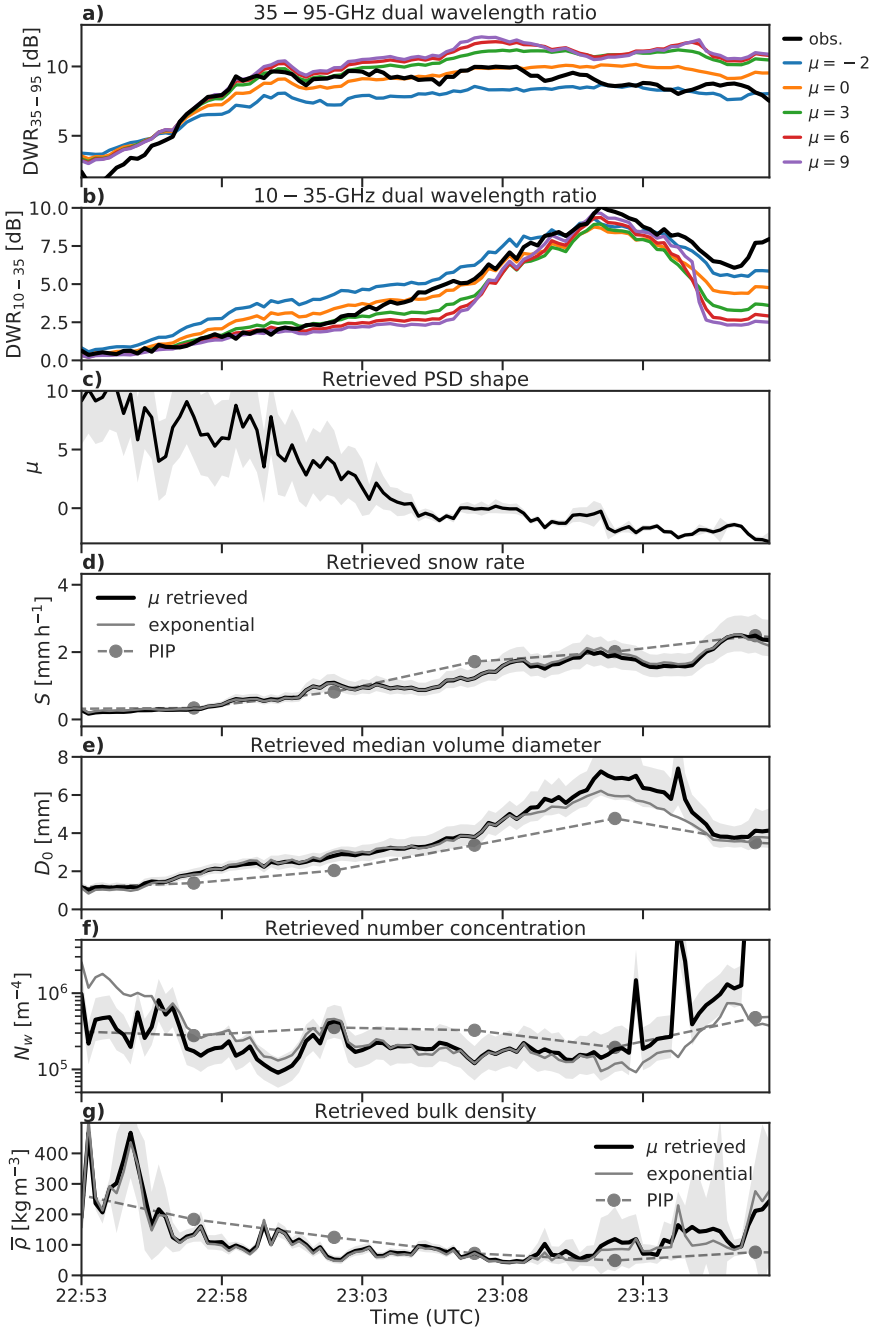

Figure 8. Measured and forward-modelled (a) DWR_{35-95} and (b) DWR_{10-35} at 500 m above ground level for CAPTIVATE retrievals assuming a range of PSD types; (c) the retrieved PSD shape compared against that estimated from in situ measurements at the surface by PIP; and (d) snow rate, (e) median volume diameter, (f) normalised number concentration, and (g) bulk density comparing values for the pseudo-retrieval against one in which exponential PSDs are assumed. Shaded regions represent the uncertainty in the retrieved values.

The potential to use advanced radar measurements to constrain ice particle properties in retrievals is of significant interest for reducing uncertainties in remote-sensed estimates of ice water content and snowfall, as well as improving understanding of the microphysics of ice and mixed-phase cloud. Two recent studies have used triple-frequency airborne radar measurements to constrain retrievals of ice particle density by modifying the prefactor of the mass-size distribution (Leinonen et al., 2018; Tridon et al., 2019); however, both studies found that triple-frequency radar retrievals were not substantially different from dual-frequency retrievals, suggesting that the problem was over-constrained. An alternative approach to estimating ice particle properties has been to use Doppler velocity as a constraint on particle density (Szyrmer and Zawadzki, 2014a; Mason et al., 2018). In this study we have built upon dual-frequency Doppler retrievals using the CAPTIVATE optimal estimation framework in which ice particle density, shape and microphysical structure are parameterized to represent a continuum of ice particles from unrimed aggregate snowflakes to dense graupel and hail (Mason et al., 2018). To our knowledge the present study is the first demonstration of a triple-frequency Doppler radar retrieval of the properties of snow particles. We found that varying the PSD shape to fit that measured in situ allowed for a retrieval in which the profiles of radar reflectivity measured at all three frequencies could be accurately represented—that is, only when non-exponential PSDs were permitted did the state space include a solution that satisfied the radar measurements at all three frequencies. From an ensemble of retrievals assuming a range of PSD shapes, a pseudo-retrieval was made of the PSD shape that best fit the triple-frequency radar measurements. This yielded an estimate of PSD shape, median volume diameter and normalized number concentration which compared well with in situ measurements at the surface;however, more accurate estimates of PSD shape had only a weak effect on the retrieved snow rate when compared with retrievals assuming an exponential PSD. Furthermore, even when the PSD shape was well-represented, triple-frequency radar measurements did not provide an adequate constraint on the density of ice particles compared with that provided by mean Doppler velocity. This supports the approach of combining Doppler and multiple-frequency radar measurements to most thoroughly characterise both the size distribution and morphology of ice particles.

The sensitivity of triple-frequency radar signatures to the shape of the PSD suggests a need to represent non-exponential PSDs within multiple-radar retrievals, but the importance of spectral features to triple-frequency radar measurements may also require an evaluation of the suitability of the Gamma distribution for representing PSDs. The shape factor of the Gamma PSD provides a convenient means of modifying the width of the PSD; however, in situ measurements of ice clouds have supported the use of modified distributions to allow for more complex size spectra (e.g. Delanoë et al., 2005; Field et al., 2005, 2007), which can also be implemented within CAPTIVATE (Mason et al., 2018). In a recent study, Grecu et al. (2018) demonstrated a retrieval of ice water content and median diameter from airborne triple-frequency radars in which the estimation was informed by a database of PSDs measured in situ, rather than assuming parameterised PSDs. Consistent with the findings of the present study, they found that including natural variability in particle spectra resulted in greater ambiguity between the triple-frequency radar signatures of different particle types than may be expected from studies assuming exponential PSDs for all particles (e.g. Kneifel et al., 2011; Leinonen and Szyrmer, 2015).

We have made a remotely-sensed estimate of PSD shape using a pseudo-retrieval that minimises the error in triple-frequency radar measurements from an ensemble of retrievals; however, future work should focus on expanding the state space to include the PSD shape within the optimal estimation framework. CAPTIVATE has been developed for retrievals from the EarthCARE

Atmos. Meas. Tech. Discuss., https://doi.org/10.5194/amt-2019-100
Manuscript under review for journal Atmos. Meas. Tech.
Discussion started: 18 March 2019

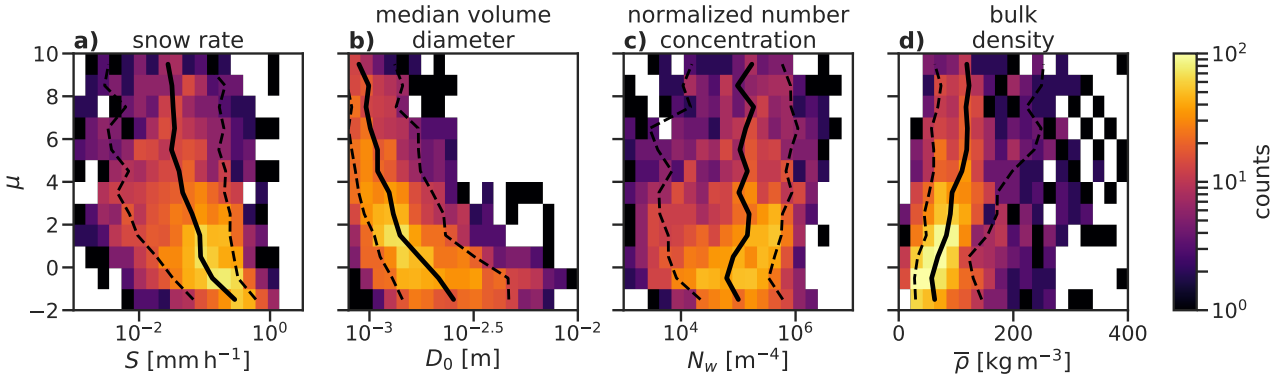

Figure 9. Joint histograms of (a) snow rate, (b) median volume diameter, (c) normalized number concentration and (d) bulk density against PSD shape μ from 2 years of PIP observations taken at Hyytiälä, Finland (von Lerber et al., 2017). Solid black lines mark the median of the respective quantities for each value of PSD shape; dashed lines mark the 10th and 90th percentiles of the distribution.

94-GHz Doppler cloud profiling radar in synergy with lidar and radiometers (Illingworth et al., 2015), and while it provides the flexibility to assimilate measurements from multiple radars and modify the state vector to parameterise ice particle properties, PSD shape is not currently configurable as a state variable. Retrieving PSD shape within the optimal estimation framework would have the advantages of permitting an a priori assumption of exponential PSDs when triple-frequency measurements provide little information, of quantifying uncertainties in the retrieved PSD shape, and of allowing changes in PSD shape to be resolved through the profile. Estimates of all three parameters of a Gamma PSD and their associated uncertainties would contribute to studies using advanced remote sensing to better observe the relationship between particle properties and microphysical processes (Mace and Benson, 2017; Mason et al., 2018).

In the present configuration of CAPTIVATE it was found that triple-frequency radar measurements could be used to retrieve three parameters of the PSD, but they were a relatively weak constraint on the density, shape and structure of the ice particles—the parameterisation of which was formulated to be constrained by Doppler velocity information (Mason et al., 2018). The low sensitivity of the retrieved particle density to triple-frequency radar measurements may be because the rimed snow in this case comprised compact graupel-like particles with median volume diameters near the limit for the onset of non-Rayleigh scattering at 95-GHz. Given the well-established links between particle morphology and triple-frequency measurements, the use of triple-frequency radar signatures to retrieve ice particle properties should not be ruled out; retrievals of cases featuring the riming of larger aggregates may find that the triple-frequency radar measurements provide a stronger constraint on particle density. In the case studied here there is a strong association between PSD shape and particle morphology, with the prefrontal regime characterised by a narrow distribution of graupel-like particles, and the frontal regime by a broad PSD dominated by large aggregate snowflakes. Two winters of the properties of snow at Hyytiälä from the retrieval of von Lerber et al. (2017, Fig. 9) show that narrower PSDs are consistently associated with light snowfall dominated by smaller and denser particles, while broad PSDs are associated with the heaviest snowfall and dominated by large, low-density snowflakes. The tendency of

heavily rimed snow and graupel to have narrower size distributions is consistent with other observations (Garrett et al., 2015); however, Tiira et al. (2016) found only a weak relation between ice bulk density and PSD shape measured at Hyytiälä. Some studies have linked PSD shape to median volume diameter or a spectral width parameter (Williams et al., 2014), a method which may be especially suited to studies combining triple-frequency and Doppler spectral information (Kneifel et al., 2016); however, correlations between PSD parameters measured by distrometers must be treated with caution due to the possibility of statistical artefacts due to spectral truncation (Moisseev and Chandrasekar, 2007). Further in situ measurements from a variety of locations are needed to study the processes linking PSD shape with particle morphology, and will be critical to maximising the use of triple-frequency radar signatures in retrievals.

We have demonstrated a novel method using triple-frequency Doppler radar measurements from the snow experiment intensive observation period of the BAECC 2014 campaign in Hyytiälä, Finland. The simultaneous retrieval of the size distribution and morphology of ice particles is only possible due to the availability of high-quality remotely-sensed measurements supported by in situ observations at the surface (Tiira et al., 2016; von Lerber et al., 2017; Moisseev et al., 2017), and in a location where wintertime precipitation is frequently not affected by melting. The significant challenges of colocating and cross-calibrating multiple radars, and of correcting for attenuation due to supercooled liquid water, have been addressed by Kneifel et al. (2015); any of these effects have the potential to introduce significant biases and uncertainties in the retrieval, reinforcing the need for high quality in situ measurements. The scarcity of such high quality datasets, their importance for evaluating our models of ice particle morphology and size distribution, and for testing retrievals against in situ measurements, make the case for further and ongoing deployments of multiple-frequency Doppler radar instruments at a range of ARM and Cloudnet field sites.

Insights into ice and mixed-phase microphysics triple-frequency Doppler radar retrievals may inform particle models used in retrievals with fewer radar frequencies, such as to the 94-GHz Doppler cloud profile radar aboard EarthCARE (Illingworth et al., 2015). In planning for satellite missions beyond EarthCARE (National Academies of Sciences Engineering and Medicine, 2018), the benefits of dual-frequency radar as a constraint on size and number concentration of hydrometeors has been well-established (e.g. Leinonen et al., 2018; Mason et al., 2017, 2018). As a constraint on the retrieval of particle density, triple-frequency radar has thus far provided relatively small advantages over dual-frequency radars (Leinonen et al., 2018; Tridon et al., 2019) when compared with Doppler velocity (Mason et al., 2018); however, we have demonstrated that triple-frequency radar measurements can be used to constrain additional properties of the PSD to provide insights into ice and mixed-phase cloud microphysics.

References

Battaglia, A. and Delanoë, J.: Synergies and complementarities of CloudSat-CALIPSO snow observations, Journal of Geophysical Research: Atmospheres, 118, 721–731, https://doi.org/10.1029/2012JD018092, http://doi.wiley.com/10.1029/2012JD018092, 2013.

Brown, P. R. A. and Francis, P. N.: Improved Measurements of the Ice Water Content in Cirrus Using a Total-Water Probe, Journal of Atmospheric and Oceanic Technology, 12, 410–414, 1995.

Delanoë, J., Protat, A., Testud, J., Bouniol, D., Heymsfield, A. J., Bansemer, A., Brown, P. R. A., and Forbes, R. M.: Statistical properties of the normalized ice particle size distribution, Journal of Geophysical Research, 110, D10 201, https://doi.org/10.1029/2004JD005405, http://doi.wiley.com/10.1029/2004JD005405, 2005.

Delanoë, J. M. E. and Hogan, R. J.: A variational scheme for retrieving ice cloud properties from combined radar, lidar, and infrared radiometer, Journal of Geophysical Research, 113, D07 204, https://doi.org/10.1029/2007JD009000, http://onlinelibrary.wiley.com/doi/10.1029/2007JD009000/fullhttp://doi.wiley.com/10.1029/2007JD009000, 2008.

Field, P. R., Hogan, R. J., Brown, P. R. A., Illingworth, A. J., Choularton, T. W., and Cotton, R. J.: Parametrization of ice-particle size distributions for mid-latitude stratiform cloud, Quarterly Journal of the Royal Meteorological Society, 131, 1997–2017, https://doi.org/10.1256/qj.04.134, http://doi.wiley.com/10.1256/qj.04.134, 2005.

Field, P. R., Heymsfield, A. J., and Bansemer, A.: Snow Size Distribution Parameterization for Midlatitude and Tropical Ice Clouds, Journal of the Atmospheric Sciences, 64, 4346–4365, https://doi.org/10.1175/2007JAS2344.1, http://journals.ametsoc.org/doi/abs/10.1175/2007JAS2344.1, 2007.

Garrett, T. J., Yuter, S. E., Fallgatter, C., Shkurko, K., Rhodes, S. R., and Endries, J. L.: Orientations and aspect ratios of falling snow, Geophysical Research Letters, 42, 4617–4622, https://doi.org/10.1002/2015GL064040, http://doi.wiley.com/10.1002/2015GL064040, 2015.

Grazioli, J., Lloyd, G., Panziera, L., Hoyle, C. R., Connolly, P. J., Henneberger, J., and Berne, A.: Polarimetric radar and in situ observations of riming and snowfall microphysics during CLACE 2014, Atmospheric Chemistry and Physics, 15, 13 787–13 802, https://doi.org/10.5194/acp-15-13787-2015, http://www.atmos-chem-phys.net/15/13787/2015/, 2015.

Grecu, M., Tian, L., Heymsfield, G. M., Tokay, A., Olson, W. S., Heymsfield, A. J., and Bansemer, A.: Nonparametric Methodology to Estimate Precipitating Ice from Multiple-Frequency Radar Reflectivity Observations, Journal of Applied Meteorology and Climatology, 57, 2605–2622, https://doi.org/10.1175/JAMC-D-18-0036.1, http://journals.ametsoc.org/doi/10.1175/JAMC-D-18-0036.1, 2018.

Hogan, R. J.: A Variational Scheme for Retrieving Rainfall Rate and Hail Reflectivity Fraction from Polarization Radar, Journal of Applied Meteorology and Climatology, 46, 1544–1564, https://doi.org/10.1175/JAM2550.1, http://journals.ametsoc.org/doi/abs/10.1175/JAM2550.1http://journals.ametsoc.org/doi/abs/10.1175/JAM2550.1, 2007.

Hogan, R. J. and Westbrook, C. D.: Equation for the Microwave Backscatter Cross Section of Aggregate Snowflakes Using the Self-Similar Rayleigh-Gans Approximation, Journal of the Atmospheric Sciences, 71, 3292–3301, https://doi.org/10.1175/JAS-D-13-0347.1, http://journals.ametsoc.org/doi/abs/10.1175/JAS-D-13-0347.1, 2014.

Hogan, R. J., Tian, L., Brown, P. R. A., Westbrook, C. D., Heymsfield, A. J., and Eastment, J. D.: Radar Scattering from Ice Aggregates Using the Horizontally Aligned Oblate Spheroid Approximation, Journal of Applied Meteorology and Climatology, 51, 655–671, https://doi.org/10.1175/JAMC-D-11-074.1, http://journals.ametsoc.org/doi/abs/10.1175/JAMC-D-11-074.1, 2012.

Hogan, R. J., Honeyager, R., Tyynelä, J., and Kneifel, S.: Calculating the millimetre-wave scattering phase function of snowflakes using the self-similar Rayleigh-Gans Approximation, Quarterly Journal of the Royal Meteorological Society, 143, 834–844, https://doi.org/10.1002/qj.2968, http://doi.wiley.com/10.1002/qj.2968, 2017.

Illingworth, A. J. and Blackman, T. M.: The Need to Represent Raindrop Size Spectra as Normalized Gamma Distributions for the Interpretation of Polarization Radar Observations, Journal of Applied Meteorology, 41, 286–297, https://doi.org/10.1175/1520-0450(2002)041<0286:TNTRRS>2.0.CO;2, http://journals.ametsoc.org/doi/abs/10.1175/1520-0450(2002)041<0286:TNTRRS>2.0.CO;2, 2002.

Illingworth, A. J., Barker, H. W., Beljaars, A., Ceccaldi, M., Chepfer, H., Clerbaux, N., Cole, J., Delanoë, J., Domenech, C., Donovan, D. P., Fukuda, S., Hirakata, M., Hogan, R. J., Huenerbein, A., Kollias, P., Kubota, T., Nakajima, T., Nakajima, T. Y., Nishizawa, T., Ohno, Y., Okamoto, H., Oki, R., Sato, K., Satoh, M., Shephard, M. W., Velázquez-Blázquez, A., Wandinger, U., Wehr, T., and van Zadelhoff, G.-J.: The EarthCARE Satellite: The Next Step Forward in Global Measurements of Clouds, Aerosols, Precipitation, and Radiation, Bulletin of the American Meteorological Society, 96, 1311–1332, https://doi.org/10.1175/BAMS-D-12-00227.1, http://journals.ametsoc.org/doi/abs/10.1175/BAMS-D-12-00227.1, 2015.

Kalesse, H., Szyrmer, W., Kneifel, S., Kollias, P., and Luke, E.: Fingerprints of a riming event on cloud radar Doppler spectra: observations and modeling, Atmospheric Chemistry and Physics, 16, 2997–3012, https://doi.org/10.5194/acp-16-2997-2016, http://www.atmos-chem-phys.net/16/2997/2016/, 2016.

Kneifel, S., Kulie, M. S., and Bennartz, R.: A triple-frequency approach to retrieve microphysical snowfall parameters, Journal of Geophysical Research Atmospheres, https://doi.org/10.1029/2010JD015430, 2011.

Kneifel, S., von Lerber, A., Tiira, J., Moisseev, D., Kollias, P., and Leinonen, J.: Observed relations between snowfall microphysics and triple-frequency radar measurements, Journal of Geophysical Research: Atmospheres, 120, 6034–6055, https://doi.org/10.1002/2015JD023156, http://doi.wiley.com/10.1002/2015JD023156http://onlinelibrary.wiley.com/doi/10.1002/2015JD023156/full, 2015.

Kneifel, S., Kollias, P., Battaglia, A., Leinonen, J., Maahn, M., Kalesse, H., and Tridon, F.: First observations of triple-frequency radar Doppler spectra in snowfall: Interpretation and applications, Geophysical Research Letters, 43, 2225–2233, https://doi.org/10.1002/2015GL067618, http://doi.wiley.com/10.1002/2015GL067618https://agupubs.onlinelibrary.wiley.com/doi/abs/10.1002/2015GL067618, 2016.

Kneifel, S., Dias Neto, J., Ori, D., Moisseev, D., Tyynelä, J., Adams, I. S., Kuo, K.-S., Bennartz, R., Berne, A., Clothiaux, E. E., Eriksson, P., Geer, A. J., Honeyager, R., Leinonen, J., and Westbrook, C. D.: Summer Snowfall Workshop: Scattering Properties of Realistic Frozen Hydrometeors from Simulations and Observations, as well as Defining a New Standard for Scattering Databases, Bulletin of the American Meteorological Society, 99, ES55–ES58, https://doi.org/10.1175/BAMS-D-17-0208.1, http://journals.ametsoc.org/doi/10.1175/BAMS-D-17-0208.1, 2018.

Langleben, M. P.: The terminal velocity of snowflakes, Quarterly Journal of the Royal Meteorological Society, 80, 174–181, https://doi.org/10.1002/qj.49708034404, http://doi.wiley.com/10.1002/qj.49708034404, 1954.

Leinonen, J. and Moisseev, D. N.: What do triple-frequency radar signatures reveal about aggregate snowflakes?, Journal of Geophysical Research: Atmospheres, 120, 229–239, https://doi.org/10.1002/2014JD022072, http://onlinelibrary.wiley.com/doi/10.1002/2014JD022072/fullhttp://doi.wiley.com/10.1002/2014JD022072, 2015.

Leinonen, J. and Szyrmer, W.: Radar signatures of snowflake riming: A modeling study, Earth and Space Science, 2, 346–358, https://doi.org/10.1002/2015EA000102, http://onlinelibrary.wiley.com/doi/10.1002/2015EA000102/fullhttp://doi.wiley.com/10.1002/2015EA000102, 2015.

Leinonen, J., Moisseev, D. N., Chandrasekar, V., and Koskinen, J.: Mapping Radar Reflectivity Values of Snowfall Between Frequency Bands, IEEE Transactions on Geoscience and Remote Sensing, 49, 3047–3058, https://doi.org/10.1109/TGRS.2011.2117432, https://ieeexplore.ieee.org/abstract/document/5738680/http://ieeexplore.ieee.org/document/5738680/, 2011.

Leinonen, J., Kneifel, S., Moisseev, D. N., Tyynelä, J., Tanelli, S., and Nousiainen, T.: Evidence of nonspheroidal behavior in millimeter-wavelength radar observations of snowfall, Journal of Geophysical Research: Atmospheres, 117, n/a–n/a, https://doi.org/10.1029/2012JD017680, http://doi.wiley.com/10.1029/2012JD017680, 2012.

Leinonen, J., Lebsock, M. D., Tanelli, S., Sy, O. O., Dolan, B., Chase, R. J., Finlon, J. A., von Lerber, A., and Moisseev, D.: Retrieval of snowflake microphysical properties from multifrequency radar observations, Atmospheric Measurement Techniques, 11, 5471–5488, https://doi.org/10.5194/amt-11-5471-2018, https://www.atmos-meas-tech.net/11/5471/2018/, 2018.

Li, H., Moisseev, D., and von Lerber, A.: How Does Riming Affect Dual-Polarization Radar Observations and Snowflake Shape?, Journal of Geophysical Research: Atmospheres, 123, 6070–6081, https://doi.org/10.1029/2017JD028186, http://doi.wiley.com/10.1029/2017JD028186, 2018.

Mace, G. and Benson, S.: Diagnosing Cloud Microphysical Process Information from Remote Sensing Measurements—A Feasibility Study Using Aircraft Data. Part I: Tropical Anvils Measured during TC4, Journal of Applied Meteorology and Climatology, 56, 633–649, https://doi.org/10.1175/JAMC-D-16-0083.1, http://journals.ametsoc.org/doi/10.1175/JAMC-D-16-0083.1, 2017.

Marshall, J. S. J. and Palmer, W. M. K.: The distribution of raindrops with size, Journal of Meteorology, 5, 165–166, https://doi.org/10.1175/1520-0469(1948)005<0165:TDORWS>2.0.CO;2, 1948.

Mason, S. L., Chiu, J. C., Hogan, R. J., and Tian, L.: Improved rain rate and drop size retrievals from airborne Doppler radar, Atmospheric Chemistry and Physics, 17, 11 567–11 589, https://doi.org/10.5194/acp-17-11567-2017, https://www.atmos-chem-phys.net/17/11567/2017/, 2017.

Mason, S. L., Chiu, C. J., Hogan, R. J., Moisseev, D., and Kneifel, S.: Retrievals of riming and snow density from vertically-pointing Doppler radars, Journal of Geophysical Research: Atmospheres, https://doi.org/10.1029/2018JD028603, http://doi.wiley.com/10.1029/2018JD028603, 2018.

Moisseev, D., von Lerber, A., and Tiira, J.: Quantifying the effect of riming on snowfall using ground-based observations, Journal of Geophysical Research: Atmospheres, 122, https://doi.org/10.1002/2016JD026272, http://doi.wiley.com/10.1002/2016JD026272, 2017.

Moisseev, D. N. and Chandrasekar, V.: Examination of the μ–Λ Relation Suggested for Drop Size Distribution Parameters, Journal of Atmospheric and Oceanic Technology, 24, 847–855, https://doi.org/10.1175/JTECH2010.1, 2007.

Mosimann, L.: An improved method for determining the degree of snow crystal riming by vertical Doppler radar, Atmospheric Research, 37, 305–323, https://doi.org/10.1016/0169-8095(94)00050-N, http://www.sciencedirect.com/science/article/pii/016980959400050N, 1995.

National Academies of Sciences Engineering and Medicine: Thriving on Our Changing Planet: A Decadal Strategy for Earth Observation from Space, National Academies Press, Washington, D.C., https://doi.org/10.17226/24938, https://www.nap.edu/catalog/24938, 2018.

Newman, A. J., Kucera, P. A., and Bliven, L. F.: Presenting the Snowflake Video Imager (SVI), Journal of Atmospheric and Oceanic Technology, 26, 167–179, https://doi.org/10.1175/2008JTECHA1148.1, http://journals.ametsoc.org/doi/abs/10.1175/2008JTECHA1148.1, 2009.

Petäjä, T., O'Connor, E. J., Moisseev, D., Sinclair, V. A., Manninen, A. J., Väänänen, R., von Lerber, A., Thornton, J. A., Nicoll, K., Petersen, W., Chandrasekar, V., Smith, J. N., Winkler, P. M., Krüger, O., Hakola, H., Timonen, H., Brus, D., Laurila, T., Asmi, E., Riekkola, M.-L., Mona, L., Massoli, P., Engelmann, R., Komppula, M., Wang, J., Kuang, C., Bäck, J., Virtanen, A., Levula, J., Ritsche, M., and Hickmon, N.: BAECC: A Field Campaign to Elucidate the Impact of Biogenic Aerosols on Clouds and Climate, Bulletin of the American Meteorological Society, 97, 1909–1928, https://doi.org/10.1175/BAMS-D-14-00199.1, http://journals.ametsoc.org/doi/10.1175/BAMS-D-14-00199.1, 2016.

Stein, T. H. M., Westbrook, C. D., and Nicol, J. C.: Fractal geometry of aggregate snowflakes revealed by triple-wavelength radar measurements, Geophysical Research Letters, 42, 176–183, https://doi.org/10.1002/2014GL062170, http://doi.wiley.com/10.1002/2014GL062170, 2015.

Szyrmer, W. and Zawadzki, I.: Snow Studies. Part III: Theoretical Derivations for the Ensemble Retrieval of Snow Microphysics from Dual-Wavelength Vertically Pointing Radars, Journal of the Atmospheric Sciences, 71, 1158–1170, https://doi.org/10.1175/JAS-D-12-0285.1, http://journals.ametsoc.org/doi/abs/10.1175/JAS-D-12-0285.1, 2014a.

Szyrmer, W. and Zawadzki, I.: Snow Studies. Part IV: Ensemble Retrieval of Snow Microphysics from Dual-Wavelength Vertically Pointing Radars, Journal of the Atmospheric Sciences, 71, 1171–1186, https://doi.org/10.1175/JAS-D-12-0286.1, http://journals.ametsoc.org/doi/abs/10.1175/JAS-D-12-0286.1, 2014b.

Testud, J., Oury, S., Black, R. A., Amayenc, P., and Dou, X.: The Concept of "Normalized" Distribution to Describe Raindrop Spectra: A Tool for Cloud Physics and Cloud Remote Sensing, Journal of Applied Meteorology, 40, 1118–1140, https://doi.org/10.1175/1520-0450(2001)040<1118:TCONDT>2.0.CO;2, http://journals.ametsoc.org/doi/abs/10.1175/1520-0450(2001)040<1118:TCONDT>2.0.CO;2, 2001.

Tiira, J., Moisseev, D. N., von Lerber, A., Ori, D., Tokay, A., Bliven, L. F., and Petersen, W.: Ensemble mean density and its connection to other microphysical properties of falling snow as observed in Southern Finland, Atmospheric Measurement Techniques, 9, 4825–4841, https://doi.org/10.5194/amt-9-4825-2016, http://www.atmos-meas-tech.net/9/4825/2016/, 2016.

Tridon, F., Battaglia, A., Chase, R. J., Truk, F. J., Leinonen, J., Kneifel, S., Mroz, K., Finlon, J., Bansemer, A., Tanelli, S., Heymsfield, A. J., and Nesbitt, S. W.: The microphysics of stratiform precipitation during OLYMPEx:compatibility between 3-frequency radar and airborne in situ observations, Journal of Geophysical Research: Atmospheres, 2019.

von Lerber, A., Moisseev, D., Bliven, L. F., Petersen, W., Harri, A.-M., and Chandrasekar, V.: Microphysical Properties of Snow and Their Link to Ze-S Relations during BAECC 2014, Journal of Applied Meteorology and Climatology, 56, 1561–1582, https://doi.org/10.1175/JAMC-D-16-0379.1, http://journals.ametsoc.org/doi/10.1175/JAMC-D-16-0379.1, 2017.

Westbrook, C. D., Ball, R. C., Field, P. R., and Heymsfield, A. J.: Universality in snowflake aggregation, Geophysical Research Letters, 31, L15 104, https://doi.org/10.1029/2004GL020363, http://doi.wiley.com/10.1029/2004GL020363, 2004.

Williams, C. R., Bringi, V. N., Carey, L. D., Chandrasekar, V., Gatlin, P. N., Haddad, Z. S., Meneghini, R., Joseph Munchak, S., Nesbitt, S. W., Petersen, W. A., Tanelli, S., Tokay, A., Wilson, A., Wolff, D. B., Williams, C. R., Bringi, V. N., Carey, L. D., Chandrasekar, V., Gatlin, P. N., Haddad, Z. S., Meneghini, R., Munchak, S. J., Nesbitt, S. W., Petersen, W. A., Tanelli, S., Tokay, A., Wilson, A., and Wolff, D. B.: Describing the Shape of Raindrop Size Distributions Using Uncorrelated Raindrop Mass Spectrum Parameters, Journal of Applied Meteorology and Climatology, 53, 1282–1296, https://doi.org/10.1175/JAMC-D-13-076.1, http://journals.ametsoc.org/doi/abs/10.1175/JAMC-D-13-076.1, 2014.

Data availability. AMF2 remote-sensed data from BAECC 2014 are available from the ARM data archive (https://www.arm.gov/data). PIP video disdrometer measurements from Hyytiälä can be accessed at github (https://github.com/dmoisseev/Snow-Retrievals-2014-2015).

Atmos. Meas. Tech. Discuss., https://doi.org/10.5194/amt-2019-100
Manuscript under review for journal Atmos. Meas. Tech.
Discussion started: 18 March 2019

Atmospheric Measurement Techniques Discussions

Appendix A: Retrieved profiles

The profiles of retrieved variables corresponding to the retrievals described in Section 4.2 are Fig. A1 for the prefrontal regime and Fig. A2 for the frontal regime.

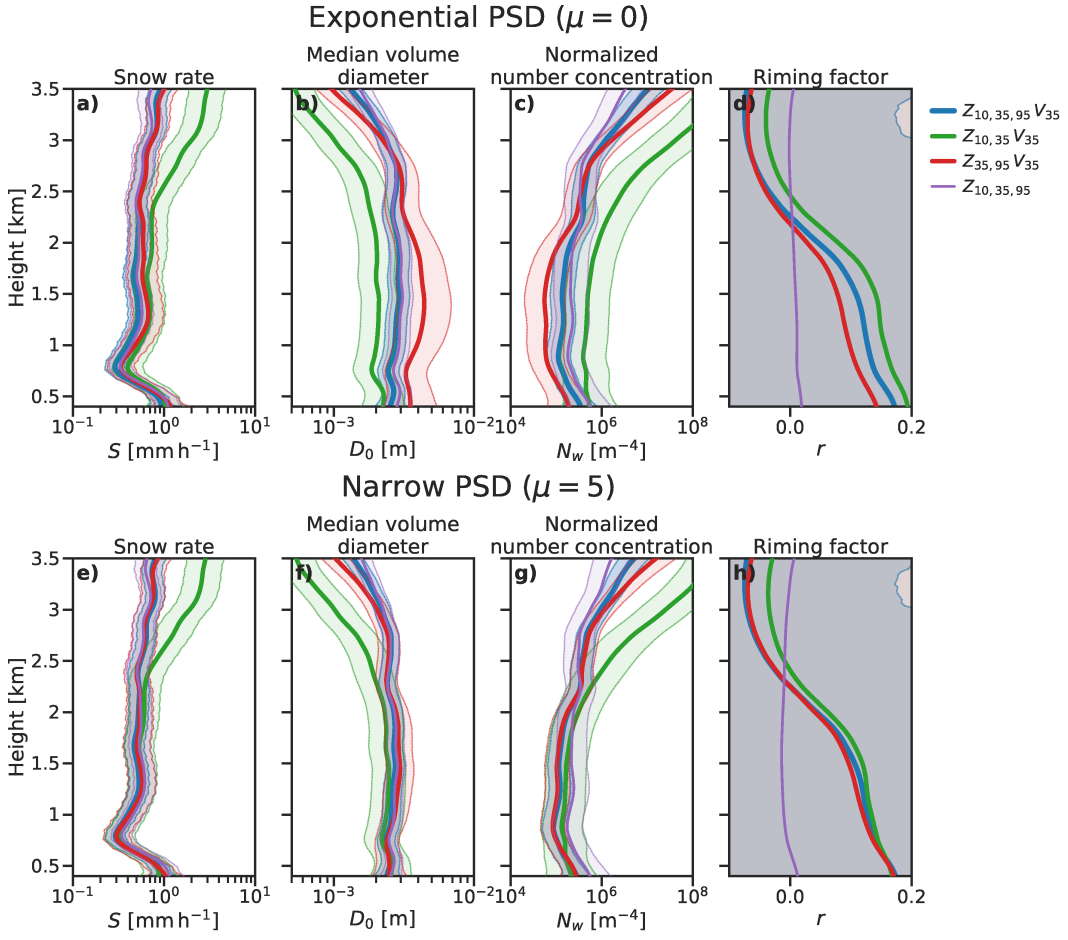

Figure A1. Profiles of retrieved variables for retrievals of a selected profile during the prefrontal snow regime. Retrievals assuming (a–d) an exponential PSD are compared against those with (e–h) a narrow PSD with $\mu = 5$.

Atmos. Meas. Tech. Discuss., https://doi.org/10.5194/amt-2019-100
Manuscript under review for journal Atmos. Meas. Tech.
Discussion started: 18 March 2019

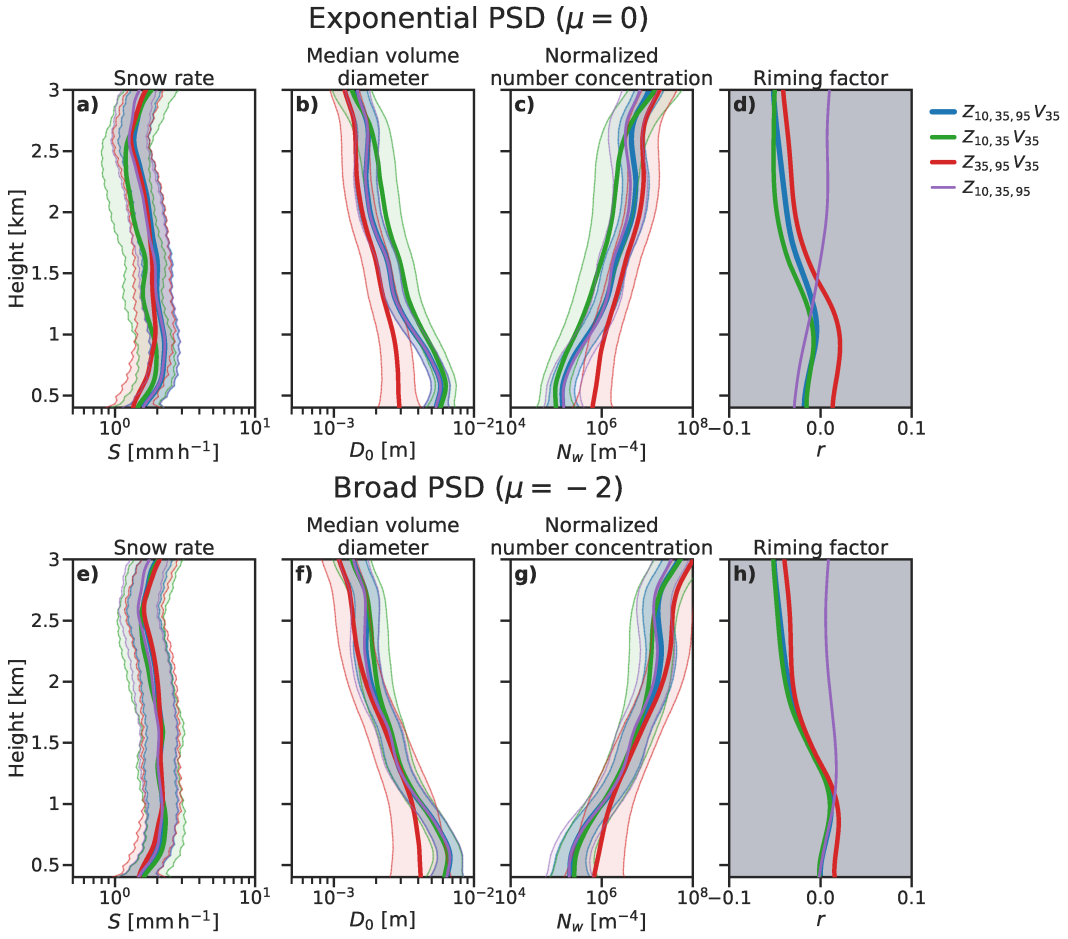

Figure A2. Profiles of retrieved variables for retrievals of a selected profile during the frontal snow regime. Retrievals assuming (a–b) an exponential PSD are compared against those with (e–h) a broad PSD with $\mu = -2$.

Competing interests. The authors do not have any competing interests.

Acknowledgements. This work is supported by the National Centre for Earth Observation (NCEO) and European Space Agency Grant 4000112030/15/NL/CT, with computing resources provided by the University of Reading. D. Moisseev acknowledges funding from ERA-PLANET, transnational project iCUPE (Grant Agreement 689443), funded under the EU Horizon 2020 Framework Programme and Academy of Finland (grants 307331 and 305175). Contributions by S. Kneifel were carried out within the Emmy-Noether Group OPTIMIce funded by the German Science Foundation (DFG) under Grant KN 1112/2-1.